# PREFABRICATED GEOSYNTHETIC DRAINS:

# CHARACTERIZATION AND IMPLEMENTATION IN MSE STRUCTURES

by

Vincent F. Gusbar

A thesis submitted to the Faculty of the University of Delaware in partial fulfillment of the requirements for the degree of Master of Civil Engineering

Spring 2006

UMI Number: 1435833

UMI Microform 1435833



ProQuest Information and Learning Company
300 North Zeeb Road
P.O. Box 1346
Ann Arbor, MI 48106-1346

**PREFABRICATED GEOSYNTHETIC DRAINS:**

**CHARACTERIZATION AND IMPLEMENTATION IN MSE STRUCTURES**

by

Vincent F. Gusbar

Approved: ____________________________________________________________
Dov Leshchinsky, Ph.D.
Professor in charge of thesis on behalf of the Advisory Committee

Approved: ____________________________________________________________
Michael J. Chajes, Ph.D.
Chair of the Department of Civil and Environmental Engineering

Approved: ____________________________________________________________
Eric W. Kaler, Ph.D.
Dean of the College of Engineering

Approved: ____________________________________________________________
Conrado M. Gempesaw II, Ph.D.
Vice Provost for Academic and International Programs

## ACKNOWLEDGMENTS

I would like to extend my utmost appreciation to my advisor Dr. Dov Leshchinsky for giving me this research opportunity and for his continued support and guidance throughout my studies at the University of Delaware.

I would also like to thank Dr. Robert Koerner and Dr. George Koerner of the Geosynthetic Institute for their superb technical guidance and assistance. It was definitely a pleasure working with them.

The financial assistance, instruction, education and materials donation of the Geosynthetic Institute, its member organizations and related institutions, and the University of Delaware made this project possible and are greatly appreciated. This project was conducted under the initiative of CPReS (Center for Polymeric Reinforced Soil).

I also in particular would like to thank my parents, family and friends for their continued support and encouragement.

## TABLE OF CONTENTS

## LIST OF TABLES

## LIST OF FIGURES

**ABSTRACT**

Failures of MSE structures are often a result of poor drainage which lead to the development of pore water pressure thus decreasing the soil strength while increasing the driving forces that act on such structures. As the demand for economical designs of earth retaining structures becomes more prevalent, particularly in the private sector, there is an ever-increasing need to implement low quality (low permeability) backfill into the reinforced zone. Hence, the frequency of failures of MSE structures is likely to increase unless the poor drainage properties of the fill material are mitigated by integrating filters such as prefabricated drains to intercept and transmit the water from behind the structure to a location where it can be properly handled.

Current performance properties and criteria of prefabricated drains are not readily available. This study reports the test results of several types of prefabricated drain products. The results show the transmissivtiy of such materials under varying normal pressures, representing soil overburden pressures, and hydraulic gradients. The experimental data shows that when transmissivity data is plotted on a semi-log scale against normal stress, a bi-linear behavior is exhibited. At a certain stress level, regardless of hydraulic gradient, there is a sharp reduction in transmissivity. At this critical stress, the drain's structure collapses and, from a practical viewpoint, it ceases to function. Consequently, this work reports the transmissivity of typical drains as well as the limit overburden pressure (or embedment depth) signifying the useful limit of such drains.

This work also shows numerically how the prefabricated drains can be integrated into MSE structures. The drainage capacity, embedment depth and a steady state flow are combined to produce a tool for the proper selection of a drain for a particular application. Parametric studies show the effectiveness of properly selected drains in increasing the stability of MSE structures.

# Chapter 1

# INTRODUCTION

In current geotechnical practices, MSE walls and slopes have increased in popularity due to their highly competitive cost and wide range applicability in providing increased slope stability (Soong and Koerner 1999). Several failures of MSE structures have occurred, however, due to improper backfill material selection in conjunction with inadequate drainage practices. If properly designed and implemented, MSE walls may be constructed using low permeability backfill materials provided that proper drainage is utilized to prevent water migration into the reinforced soil zone.

## 1.1 Cost Impact

Reinforced soil structures provide a very competitive alternative to conventional earth retaining systems due to the relative low cost reinforcement material and their ability, in some instances, to utilize on-site backfill material. According to Koerner (1998), MSE structures using geosynthetic reinforcement elements provide the most cost effective earth retention solution to wall or slope heights up to 12m. If it is possible to utilize on-site backfill material, reinforced soil structures would become all the more competitive particularly in the private sector where projects are driven mainly by economics. Figure 1.1 illustrates the cost of MSE structures relative to other conventional earth retention systems.

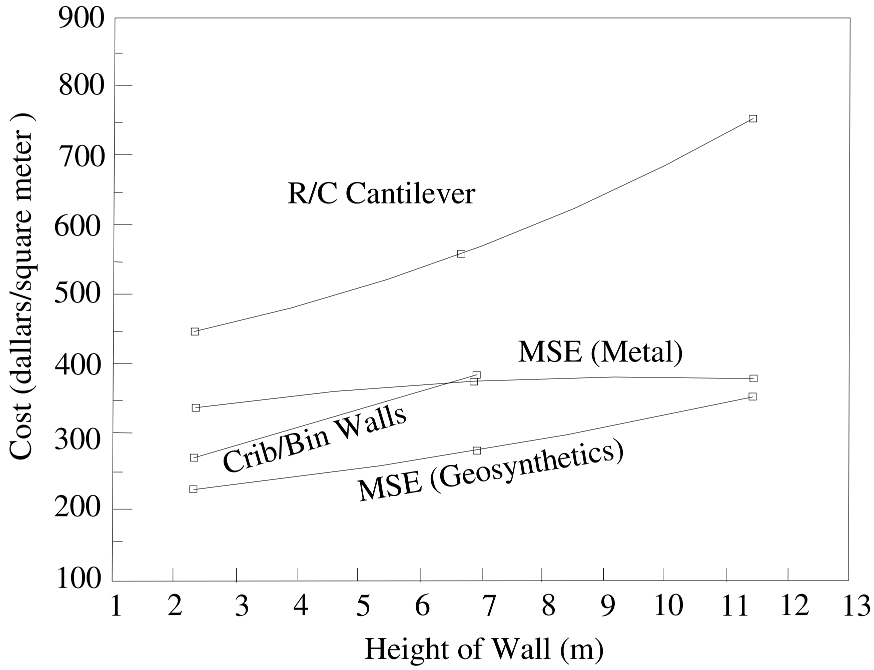


**Figure 1.1: Cost Comparison (Koerner (1998))**

The data used to generate Figure 1.1 is based on usage of high quality, high permeability backfill materials. An appropriate assumption is that the overall cost per square meter could reduce by a significant percentage if in fact on-site materials could be utilized as backfill regardless of its properties.

### 1.2 Current Design Standards

The design standards for reinforced soil structures are relatively stringent in that they limit the quality of material that may be used as the reinforced soil. According to current American Association of State Highway and Transportation Officials (AASHTO) design criteria, the reinforced backfill soil must be granular and free draining. Table 1.1 illustrates the gradation requirements for the reinforced backfill material.

**Table 1.1: Gradation Requirements (FHWA (2005))**

| Sieve Size | Percent Passing |
|---|---|
| 102mm (4in) | 100 |
| 0.425mm (No. 40) | 0-60 |
| 0.075mm (No. 200) | 0-15 |
| Plasticity Index $\leq 6$ | |

In several geographic locations the on-site soils may very well exhibit gradation other than those specified in Table 1.1 therefore requiring that more suitable material be transported from another site subsequently driving the costs of reinforced soil structures to a point where they may not be a feasible solution.

### 1.3 Soil-Water Interaction

It is well known and established in geotechnical engineering that water reduces the stability and strengths of soils. For granular soils, water effects are minimal due to their ability to drain quickly and hence develop relatively high shear strengths. However, when low permeability soils are considered, water plays a significant role in defining the overall stability. In general, water in soils introduce two problems: a) the driving forces acting on earth retaining structures increase by up to 2 times the lateral earth pressures and b) water pressure reduces the effective stresses in soil thus reducing its shear strength: this reduction can be as much as half. Subsequently, overall stability can decrease substantially by the presence of water.

### 1.4 Purpose of Study

Due to recent developments in the geosynthetic industry, the database which characterizes and compares the geosynthetic drain materials that are currently available is lacking. To design drainage systems to alleviate the effects of water it is necessary to estimate the location of the phreatic surface within a soil mass which may be difficult without the use of rigorous numerical modeling. To develop a comprehensive design procedure to implement such drains it is necessary to link drain capacity when embedded in soil, the location of the phreatic surface and the stability of the reinforced earth structure. The purpose of this thesis is to characterize several suitable geosynthetic drainage materials and to provide their implementation in reinforced earth structures in a rational way based on well established methods of design.

# Chapter 2

# EXPERIMENTAL APPROACH

## 2.1 Transmissivity Test

The experimental portion of this thesis was conducted in accordance to ASTM D4716 : *the test method for determining the in-plane flow rate per unit width and transmissivity of a geosynthetic using a constant head*. Details of this test can also be found in (Koerner 1998). The flow rate per unit width of each test specimen was determined by measuring the volume of water that passes through the specimen in a specific time interval under a specific normal stress and a specific hydraulic gradient (Koerner 2004).

## 2.2 Testing Apparatus and Setup

The testing apparatus used in this thesis consisted of a steel loading frame, plexiglass basin and testing box, outflow weir, manometers, hydraulic ram (55-ton capacity) and water pumps. Figures 2.1 through 2.3 illustrate the testing apparatus. The specimen was placed between a plexiglass plate (superstratum) and the base of the testing box. A neoprene sealing material was placed above the plexiglass plate to confine the water flow through the specimen. An aluminum plate served as the load transfer mechanism to convert the point load applied by the hydraulic ram to a normal stress over the specimen, simulating the effects of overburden pressure when the drain is embedded in soil. It was assumed that this aluminum plate experienced negligible deflections so as to apply consistent pressure to the entire specimen. A standard load cell with 20 pound graduations was utilized to measure the point load applied to the aluminum plate. The load cell was placed between the hydraulic ram and the aluminum plate. Two individual sump pumps were used to circulate the water through the system. A stand pipe on the upstream side of the specimen was used to regulate and maintain a constant head across the specimen.


**Figure 2.1: Photo of Testing Apparatus**

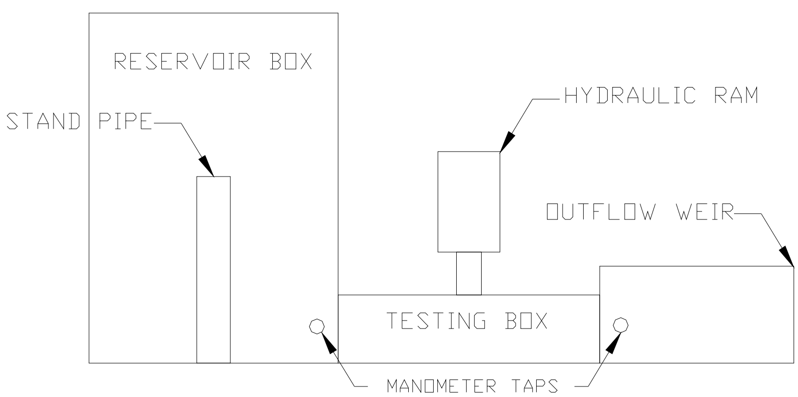


**Figure 2.2: Schematic of Testing Apparatus**

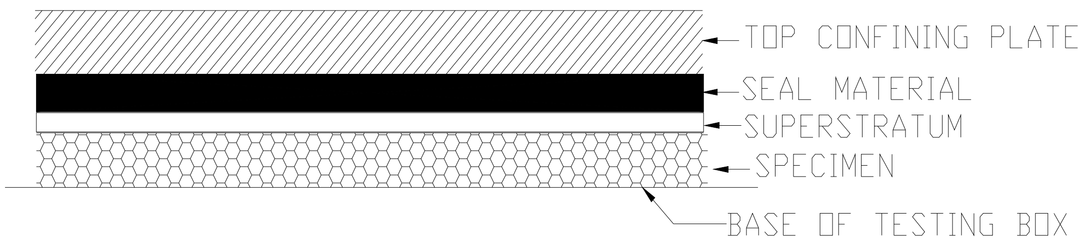


**Figure 2.3: Testing Box Detail**

A “rigid plate” setup was utilized in which no soil is placed between the upper confining plate and the geosynthetic specimen therefore measuring the nominal transmissivity of the test specimens. Representative reduction factors to account for soil intrusion, creep, and biological and chemical effects, such as recommended by Koerner and Koerner (2005), should be applied by the designer to the transmissvity test results before application to actual field conditions. The reduction factors will be discussed and detail in applied in Chapter 6.

An Internal Reference Material, commonly referred to as an “IRM” was utilized at the onset of each testing sequence to ensure the testing equipment was in proper working order as recommended by the ASTM guidelines. The IRM used in this experiment consisted of a relatively high flow capacity and high modulus tri-planar geonet.

**2.3 Testing Parameters**

Each test parameter was selected so as to represent realistic field conditions where the drain materials may be implemented. The hydraulic gradients selected can be related to the orientation of the drain as discussed later; the values selected represent nearly horizontal to a vertical installation. The normal stresses chosen represent a broad range of embedment depth in which the drainage products may be installed. The normal stress values are related to an “equivalent embedment depth” in which the applied stress, induced by the hydraulic ram, replicates either overburden or lateral earth pressures. Table 2.1 converts the applied pressure to an equivalent embedment depth exerted by a soil having a unit weight, $\gamma$, equal to $20 kN/m^3$. In certain instances when the specimen modulus appeared relatively low (i.e., the specimen compressed becoming ineffective), one test under low stress of 10kPa was added to the test parameters in order to determine the behavior of a given drain under a lighter normal stress.  Table 2.1 provides a summary of the testing parameters used in this work.

**Table 2.1: Summary of Test Parameters**

| | |
|---|---|
| Specimen Size | 0.3048m. x 0.3048m. (12in. x 12in.) |
| Hydraulic Gradient Settings | 0.1, 0.25, 0.5, 1.0 |
| Normal Stresses | 48kPa, 240kPa, 480kPa,720kPa |
| Equivalent Embedment Depth* | ≈ 2.5m, 12m, 25m, 35m |

*Based on a soil unit weight, $\gamma = 20kN/m^3$

Special care was taken to ensure the "machine direction" of the specimen was indeed oriented parallel to the direction of flow in order to determine its maximum flow capacity. This task was easily accomplished because each test material was provided in a roll in which the "machine direction" is clearly noted.

## 2.4 Testing Procedure

The testing procedures were conducted according to ASTM D4716 and commenced in the following manner:

1) Trim a minimum of four specimens to the specified dimensions;

2) Place the specimen into the testing box with the plexiglass plate installed above it (refer to Figure 2.3);

3) Install the sealing material on top of the plexiglass superstratum and apply a small amount of petroleum jelly to its perimeter to ensure a water tight seal (refer to Figure 2.3);

4) Seat the specimen under a light normal stress for a minimum of 15 minutes;

5) Engage the sump pumps and fill the upstream reservoir to maintain the initial hydraulic gradient setting;

6) Increase the normal pressure to the initial value;

7) Measure time required for a known volume of flow to pass through the specimen (repeat three times for each hydraulic gradient setting and determine their arithmetic average);

8) Repeat step 7 for each subsequent normal stress setting.

### 2.5 Materials Tested

The materials considered were submitted from several suppliers which provide a representative cross-section of drains currently available. The most common type of geosynthetic drain included a non-woven geotextile. Drains having higher flow rates such as geonets, geocomposites and sheet drains were also selected to provide a broad spectrum of material and flow characteristics for comparison.

Each geosynthetic material tested may be subdivided into one of four classifications which are illustrated in Figures 2.4 through 2.8: a) Geonets (GN); b) Geotextiles (GT-NW); c) Geocomposites (GC) and d) Sheet Drains (SD-NW, SD-W). While each product designation utilizes a unique manufacturing process, every material analyzed retains the ability to transmit fluid in the planer direction (Koerner 1998). Table 2.2 provides a summary of the materials tested.

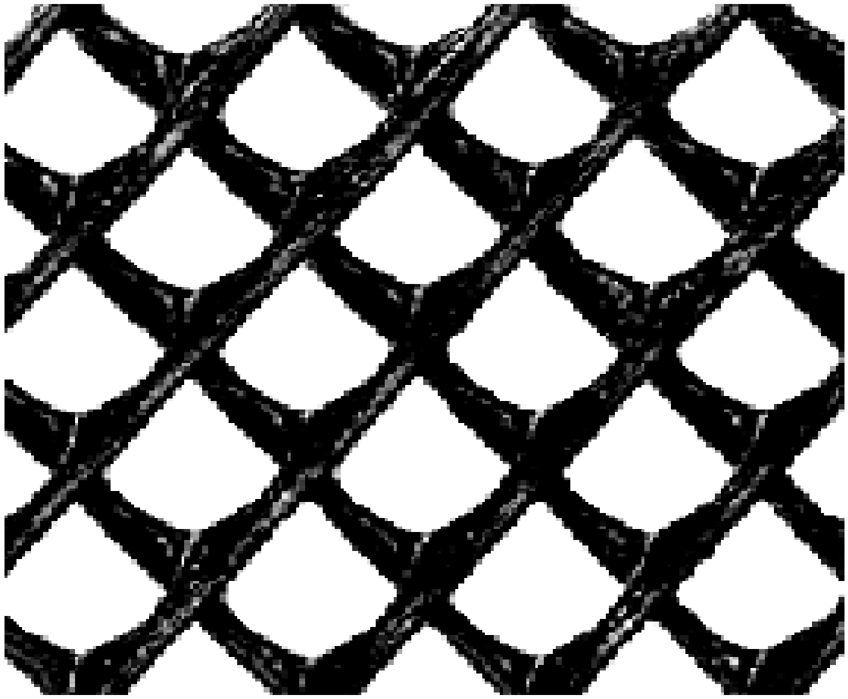

**Figure 2.4: Bi-Planar Geonet**

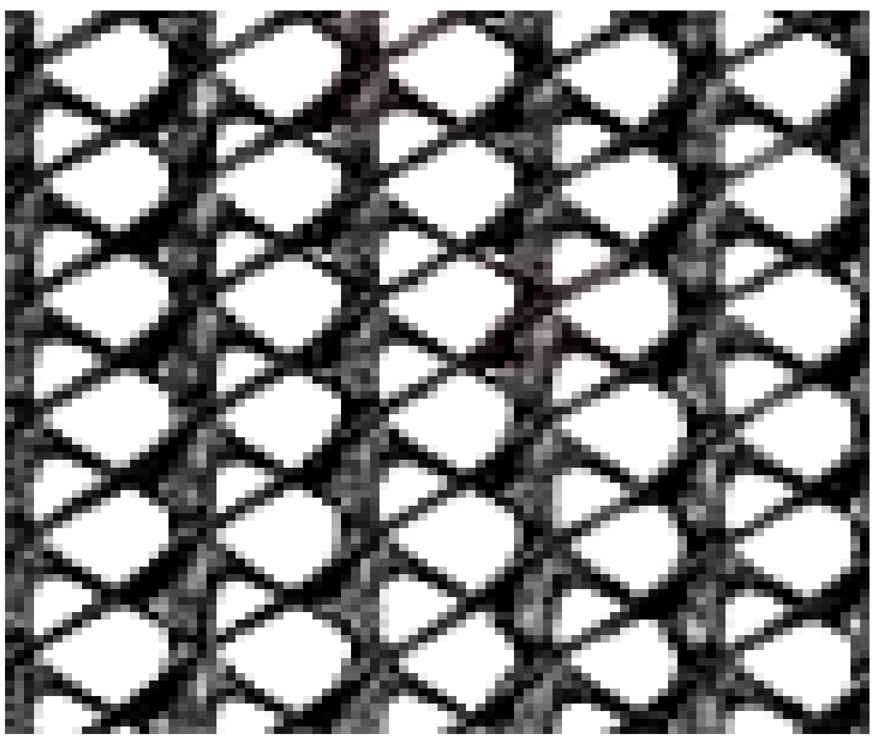

**Figure 2.5: Tri-Planar Geonet**

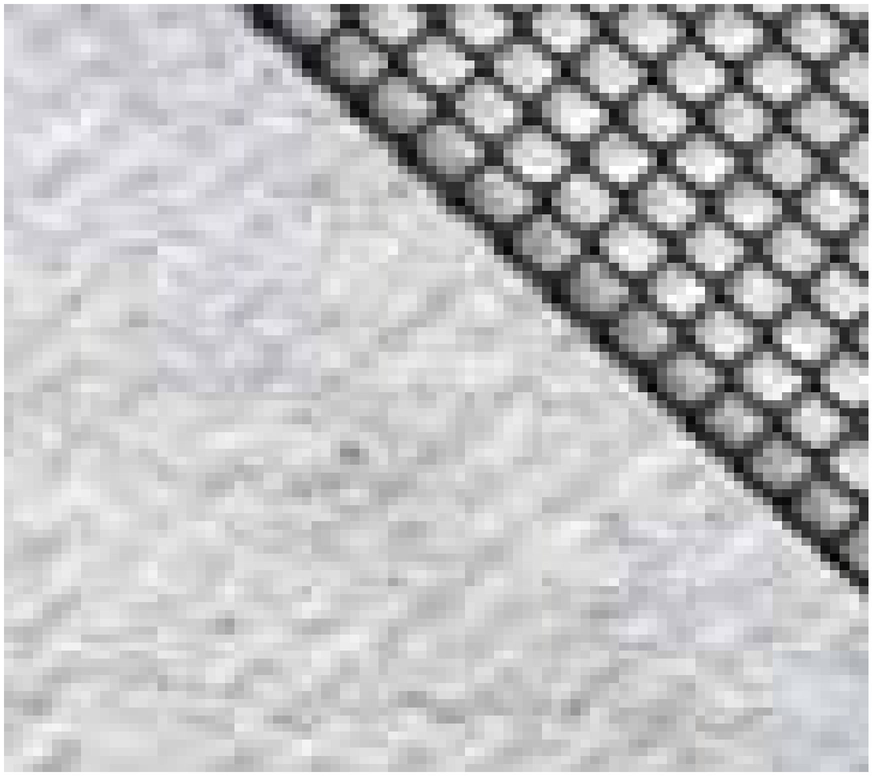

**Figure 2.6: Geocomposite with NW Geotextile Facing**

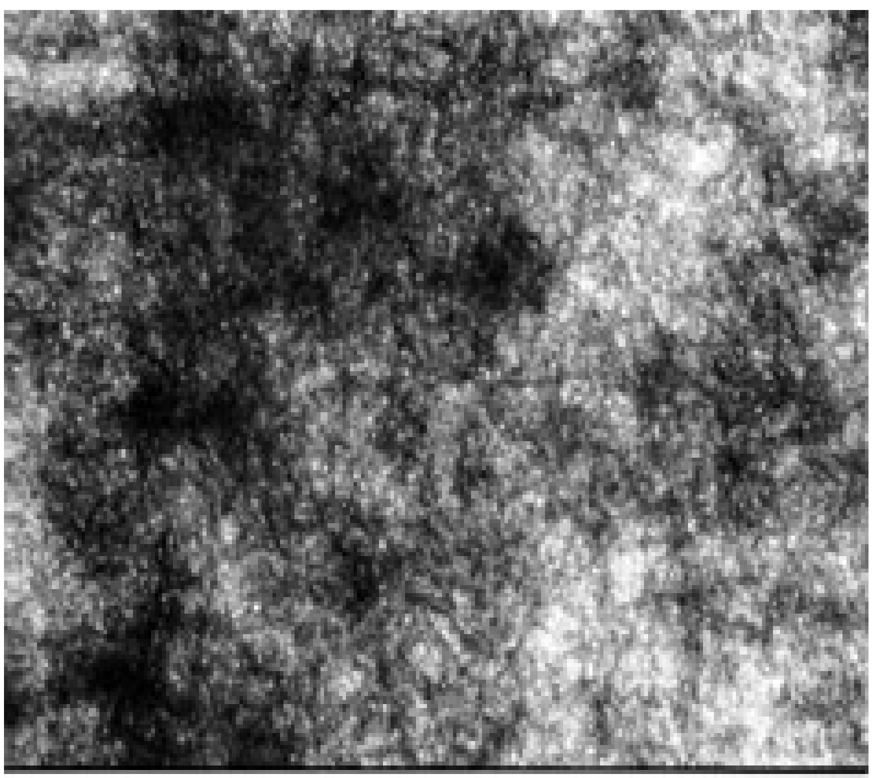

**Figure 2.7: NW Geotextile**

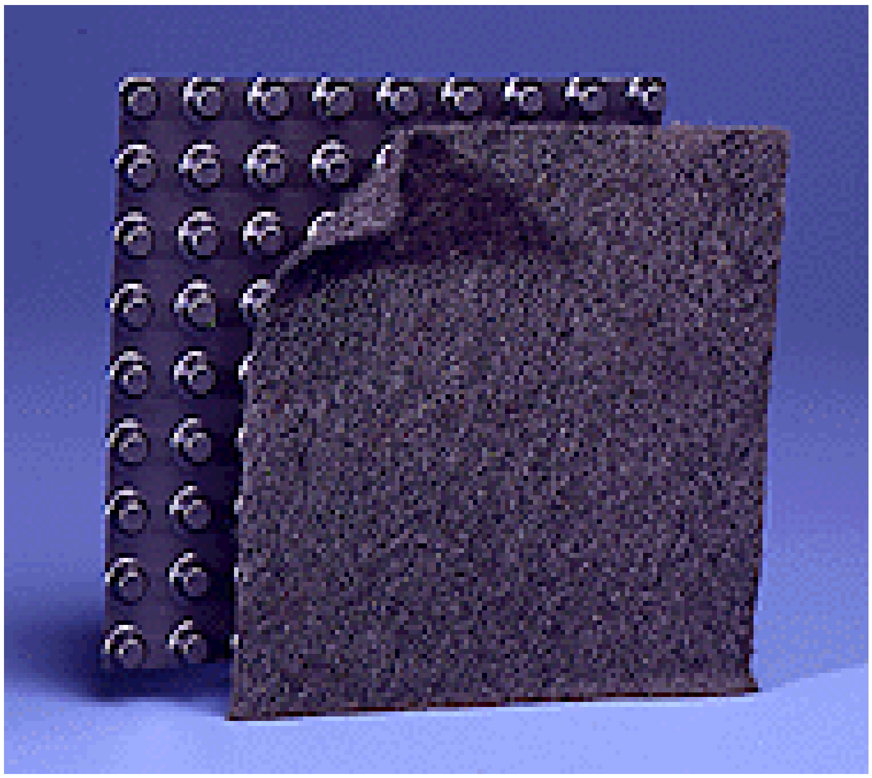

**Figure 2.8: Sheet Drain**

**Table 2.2: Summary of Materials Tested**

| Material Designation | Physical Properties | Manufacturer |
|---|---|---|
| GN (a) | Bi-Planar orientation | GSE |
| GN (b) | Tri-Planar orientation | Tenax |
| GC (a) | Nonwoven Geotextile with Bi-Planar Geonet core | GSE |
| GC (b) | Nonwoven Geotextile with Geogrid drainage core | Naue |
| GT-NW (a) | 24 oz/sqyd Non-Woven Geotextile | GSE |
| SD-NW (a) | Nonwoven Geotextile face with formed “Egg Crate” core | Ten Cate Nicolon |
| SD-NW (b) | Typar® face with formed “Egg Crate” core | Cosella-Dörken |
| SD-W (a) | Woven Geotextile face with formed “Egg Crate” core | Ten Cate Nicolon |

### 2.6 Presentation of Results

The results will be presented graphically in order to analyze how flow or transmissivity varies with an increase in normal stress. Figure 2.9 provides a schematic of the graphical data presentation used in this work.

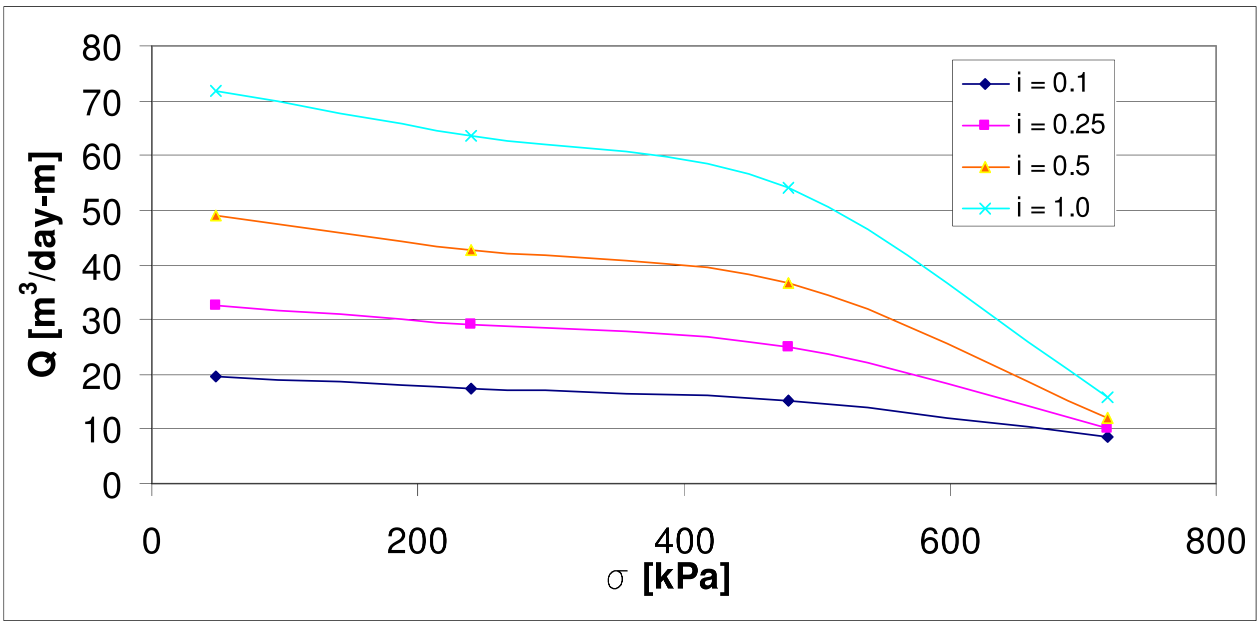


**Figure 2.9: Schematic of Graphical Data Presentation**

Transmissivity, Q, is plotted as the ordinate (y-axis) while Normal Stress, σ, is plotted as the abscissa (x-axis). Each line represents a series of tests conducted at a given hydraulic gradient. Chapter 3 will present and discuss the data rendered from each test series which will presented in the same manner as that shown in Figure 2.9.

# Chapter 3

## RESULTS OF EXPERIMENTAL PROGRAM

### 3.1 Data Parameters

The data recorded in the experimental portion of this work consisted of a time value which elapsed while a given volume of water passed through each specimen. In order to minimize experimental errors three time values were recorded which were subsequently averaged. The preset volume of water was dependent upon the relative capacity of the specimen (i.e., lower capacity specimens such as nonwoven geotextiles required a lower flow volume than higher capacity sheet drains or geonets) which was established experimentally by trial and error methods. The parameter to be calculated from the time and flow values is transmissivity and ultimately flow volume per unit time.

### 3.2 Data Reduction Procedure

The following set of equations was utilized in a tabular format to determine the respective flow rate per unit width and transmissivity values:

*Step 1: Determine Average Time Value*

$$t_{av} = \frac{1}{3}\sum t_i \qquad (1)$$

where: $t_{av}$ = average time value [sec]
$t_i$ = time value corresponding to trial i

*Step 2: Calculate the Flow Rate per Unit Width*

$$q_w = Q_t / W \qquad (2)$$

where: $q_w$ = flow rate per unit width [$m^3$/sec-m]
$Q_t$ = volume of water discharged per unit time [$m^3$/sec]
W = width of the specimen [m]

*Step 3: Determine Transmissivity*

$$\theta = \frac{q_w}{\Delta h} \qquad (3)$$

where: θ = transmissivity [$m^2$/sec]
$q_w$ = flow rate per unit width (as in Equation 2) [$m^3$/sec-m]
Δh = head difference between upstream and downstream sides of specimen (also represents hydraulic gradient) [m]

It was desirable to convert the Flow Rate per Unit Width values as determined by Equation 2 from [$m^3$/sec-m] to [$m^3$/day-m] to provide more usable results for use in design.

**3.3 Data Presentation**

Figures 3.1through 3.8 provide graphical representations of the data collected in this thesis. The material designations refer to those identified in Table 3.1. The values portrayed in these graphs include the flow rate, Q on the y-axis and the corresponding normal pressure, σ on the x-axis.

**Table 3.1: Material Designations**

| Material Designation | Physical Properties | Figure Reference |
|---|---|---|
| GN (a) | Bi-Planar orientation | 3.1 |
| GN (b) | Tri-Planar orientation | 3.2 |
| GC (a) | Nonwoven Geotextile with Bi-Planar Geonet core | 3.3 |
| GC (b) | Nonwoven Geotextile with Geogrid drainage core | 3.4 |
| GT-NW (a) | 24 oz/sqyd Non-Woven Geotextile | 3.5 |
| SD-NW (a) | Nonwoven Geotextile face with formed “Egg Crate” core | 3.6 |
| SD-NW (b) | Typar® face with formed “Egg Crate” core | 3.7 |
| SD-W (a) | Woven Geotextile face with formed “Egg Crate” core | 3.8 |

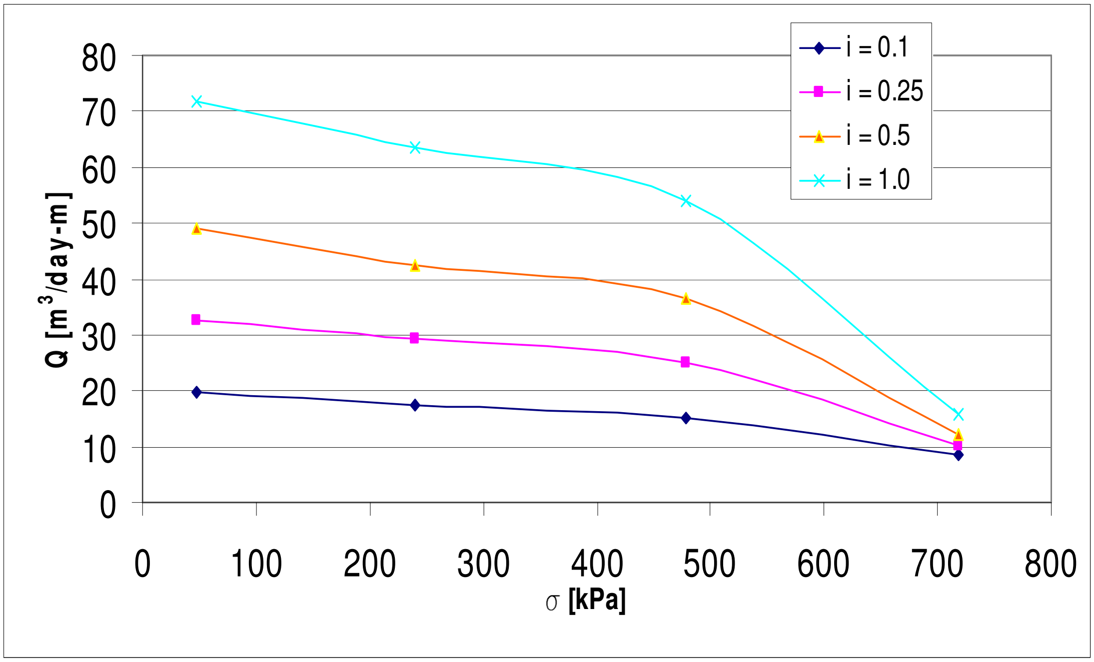


**Figure 3.1: Product GN (a)**

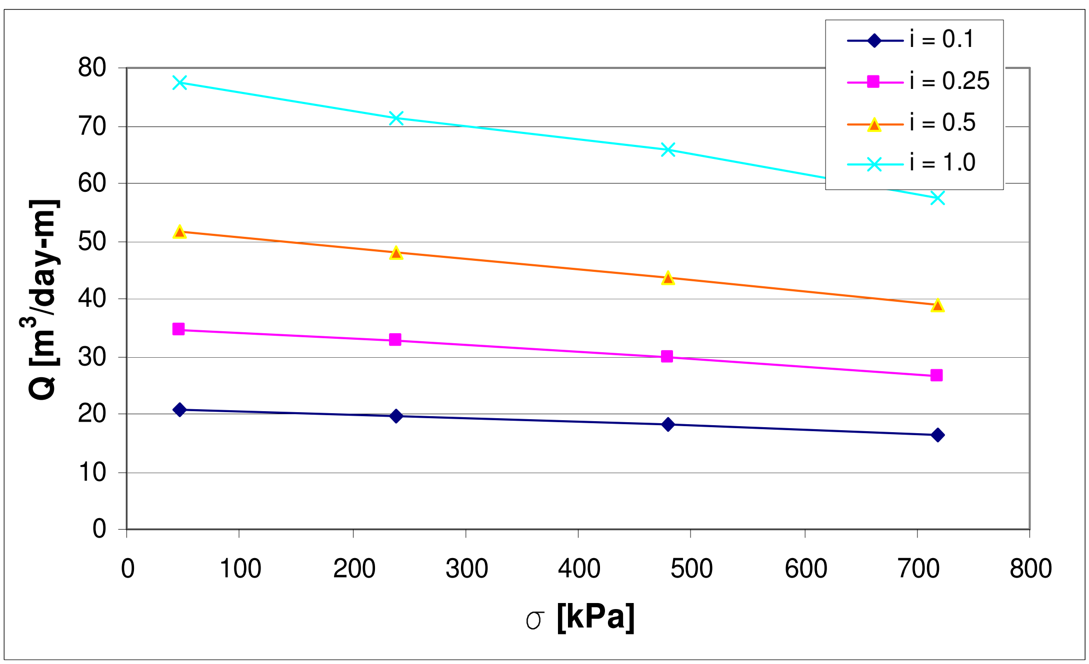


**Figure 3.2: Product GN (b)**

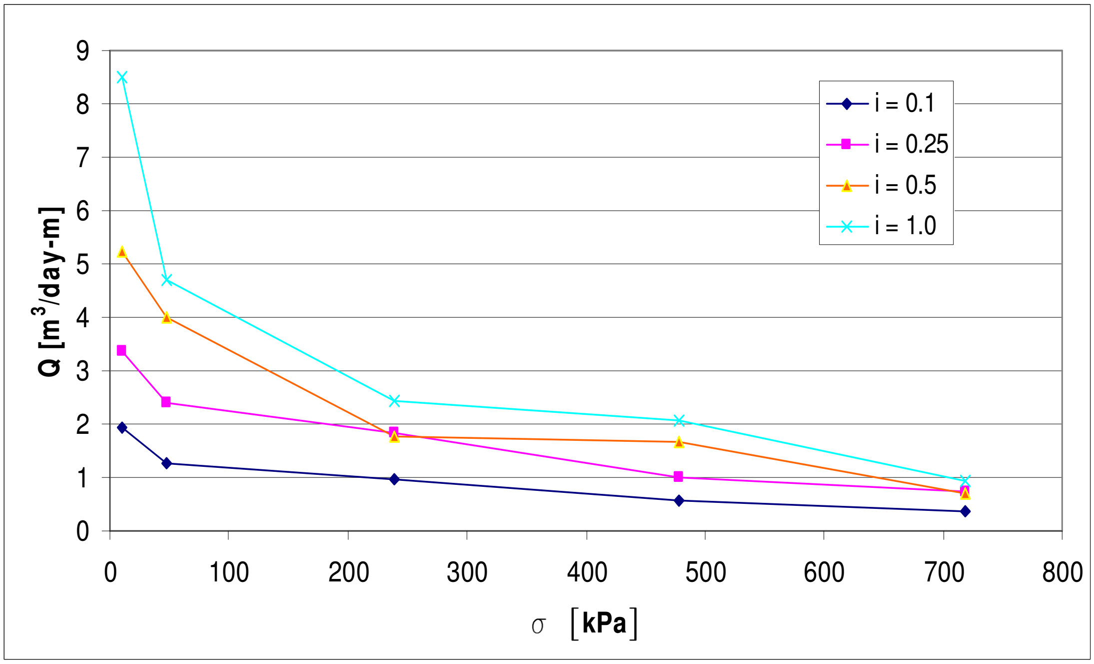


**Figure 3.3: Product GC (a)**

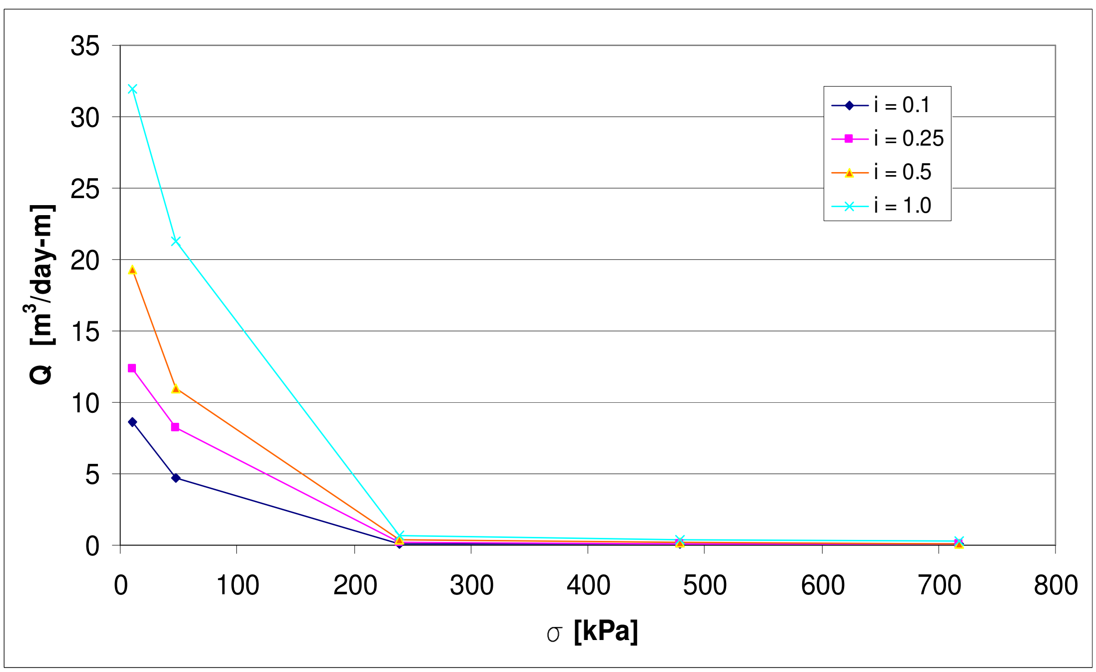


**Figure 3.4: Product GC (b)**

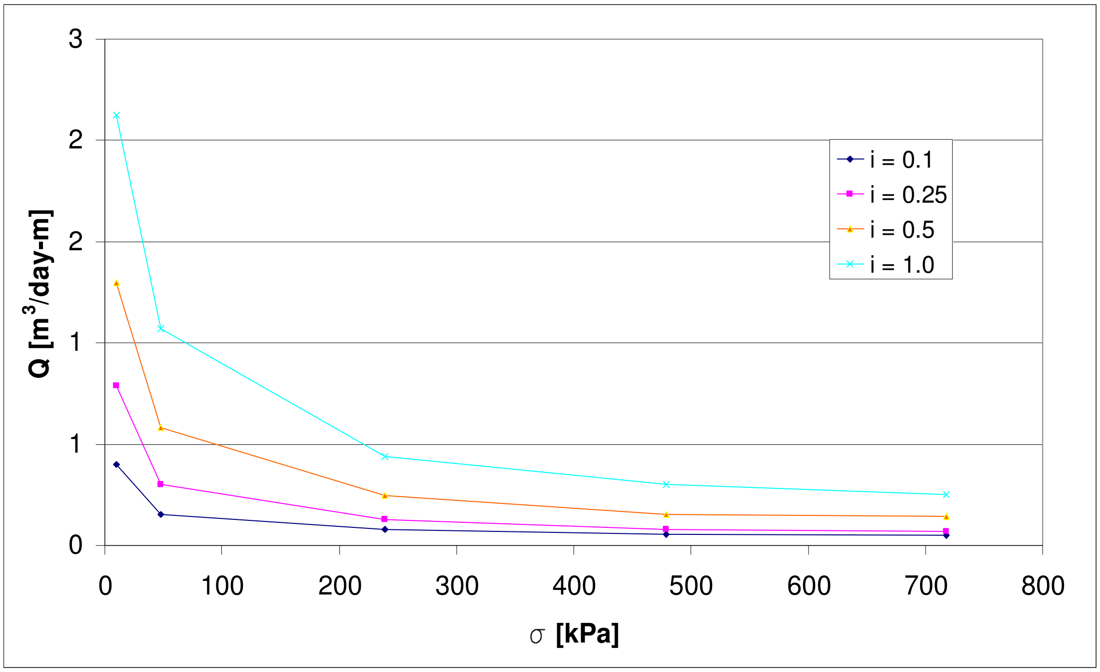


**Figure 3.5: Product GT-NW (a)**

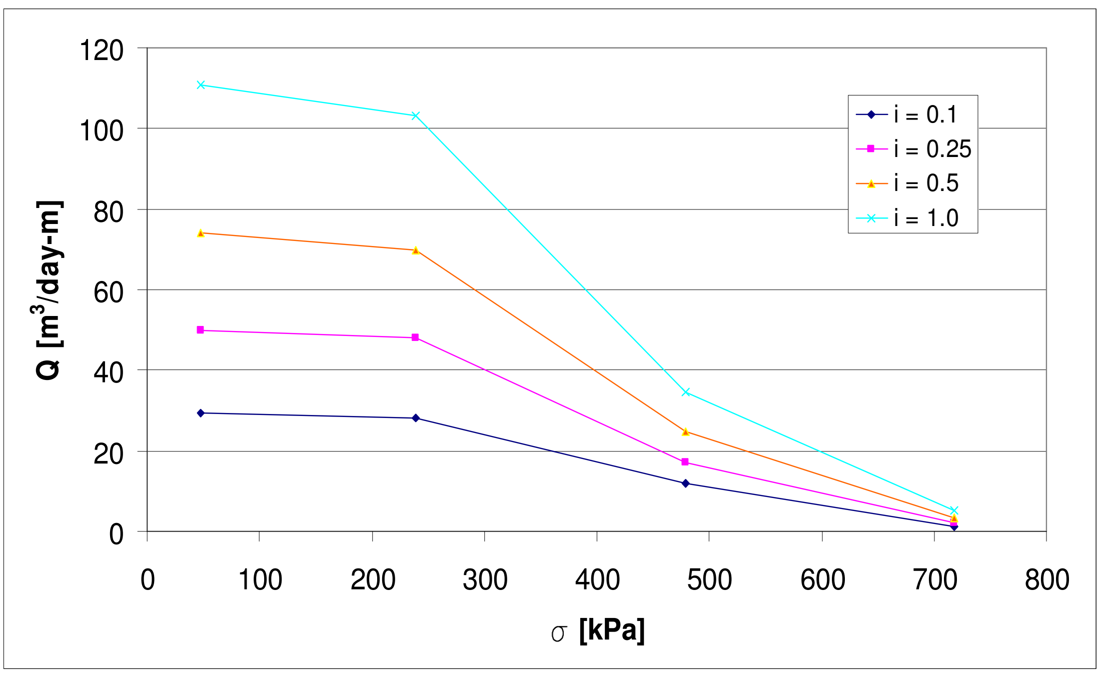


**Figure 3.6: Product SD-NW (a)**

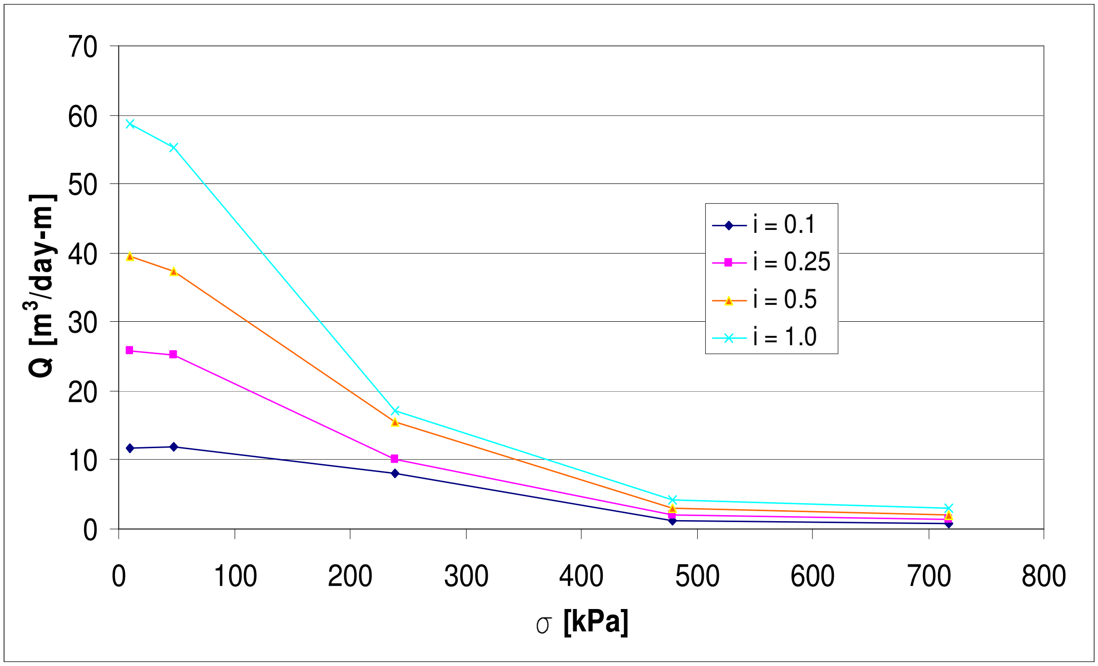


**Figure 3.7: Product SD-NW (b)**

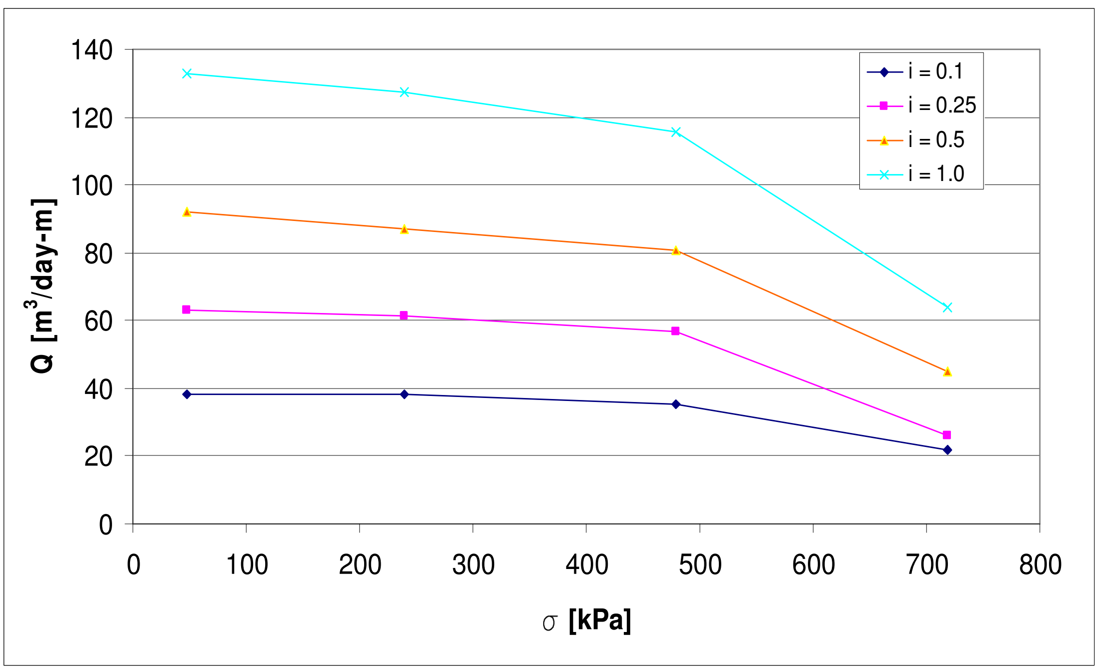


**Figure 3.8: Product SD-W (a)**

### 3.4 Discussion and Observations

Notice that in the graphical representations a definitive threshold is observed where the material no longer exhibits the ability to transmit fluid in its planer direction. Before reaching this point, a “cracking” sound was heard where structural collapse of the drain occurred. As each specimen was subjected to specified normal stresses and hydraulic gradients, a noticeable difference was observed as the stress increased. In several cases a “cracking” noise was observed as the material crushed and became virtually unusable. When this crush point is reached for each given specimen, a large quantity of short term creep was observed, it became difficult to maintain a constant normal pressure and the material demonstrated a dramatic decrease in flow capacity.

Table 3.2 summarizes the measured transmissivity, $\theta$ and flow capacity, Q for each material at each hydraulic gradient setting. The range of $\theta$ and Q illustrate the behavior of the drain from near zero confining pressure to the threshold pressure. This presentation translates the graphical representations to a numerical one which allows one to see the effect of confinement within the useable range of the drain.

## Table 3.2: Summary of Results

| Material Designation | Figure Reference | Normal Stress [kPa] | Transmissivity θ X 1,000 [$m^2$/sec] | | | | Flow Rate Q [$m^3$/day-m] | | | |
|---|---|---|---|---|---|---|---|---|---|---|
| | | | **0.1** | **0.25** | **0.5** | **1.0** | **0.1** | **0.25** | **0.5** | **1.0** |
| GN (a) | 3.1 | 48 | 7.4 | 5.0 | 3.7 | 2.7 | 19.6 | 32.7 | 48.9 | 71.8 |
| | | 240 | 6.6 | 4.4 | 3.2 | 2.4 | 17.3 | 29.1 | 42.6 | 63.6 |
| | | 480 | 5.8 | 3.8 | 2.8 | 2.1 | 15.2 | 25.1 | 36.5 | 54.1 |
| | | 720 | 4.0 | 1.9 | 1.1 | 0.68 | 8.6 | 10.2 | 12.2 | 15.8 |
| GN (b) | 3.2 | 48 | 7.8 | 5.3 | 3.9 | 2.9 | 20.6 | 34.6 | 51.8 | 77.4 |
| | | 240 | 7.4 | 4.9 | 3.6 | 2.7 | 19.5 | 32.6 | 47.9 | 71.2 |
| | | 480 | 7.0 | 4.5 | 3.3 | 2.5 | 18.4 | 29.7 | 43.6 | 65.7 |
| | | 720 | 6.3 | 4.0 | 3.0 | 2.2 | 16.5 | 26.6 | 38.9 | 57.6 |
| GC (a) | 3.3 | 10 | 0.74 | 0.51 | 0.4 | 0.32 | 1.9 | 3.4 | 5.2 | 8.5 |
| | | 48 | 0.48 | 0.36 | 0.3 | 0.14 | 1.3 | 2.4 | 4.0 | 4.7 |
| | | 240 | 0.36 | 0.28 | 0.13 | 0.092 | 1.0 | 1.8 | 1.8 | 2.4 |
| | | 480 | 0.21 | 0.15 | 0.13 | 0.078 | 0.6 | 1.0 | 1.7 | 2.1 |
| | | 720 | 0.14 | 0.11 | 0.044 | 0.035 | 0.4 | 0.7 | 0.7 | 0.9 |
| GC (b) | 3.4 | 10 | 3.3 | 1.9 | 1.5 | 1.2 | 8.6 | 12.3 | 19.3 | 31.9 |
| | | 48 | 1.8 | 1.3 | 0.83 | 0.81 | 4.7 | 8.3 | 11.0 | 21.3 |
| | | 240 | 0.044 | 0.026 | 0.028 | 0.025 | 0.1 | 0.2 | 0.4 | 0.7 |
| | | 480 | 0.028 | 0.014 | 0.015 | 0.014 | 0.1 | 0.1 | 0.2 | 0.4 |
| | | 720 | 0.02 | 0.011 | 0.0098 | 0.011 | 0.1 | 0.1 | 0.1 | 0.3 |
| GT-NW (a) | 3.5 | 10 | 0.15 | 0.12 | 0.098 | 0.081 | 0.4 | 0.79 | 1.3 | 2.1 |
| | | 48 | 0.059 | 0.045 | 0.044 | 0.041 | 0.2 | 0.3 | 0.6 | 1.1 |
| | | 240 | 0.03 | 0.019 | 0.019 | 0.017 | 0.08 | 0.13 | 0.25 | 0.44 |
| | | 480 | 0.021 | 0.012 | 0.012 | 0.011 | 0.06 | 0.08 | 0.15 | 0.3 |
| | | 720 | 0.018 | 0.01 | 0.011 | 0.009 | 0.05 | 0.07 | 0.14 | 0.25 |
| SD-NW (a) | 3.6 | 48 | 11.1 | 7.6 | 5.6 | 4.2 | 29.2 | 49.8 | 74.1 | 111.0 |
| | | 240 | 10.7 | 7.3 | 5.3 | 3.9 | 28.2 | 48.1 | 69.9 | 103.1 |
| | | 480 | 4.6 | 2.6 | 1.9 | 1.3 | 12.1 | 17.2 | 24.8 | 34.6 |
| | | 720 | 0.4 | 0.3 | 0.3 | 0.2 | 1.2 | 2.2 | 3.3 | 5.1 |
| SD-NW (b) | 3.7 | 10 | 4.5 | 3.9 | 3.0 | 2.2 | 11.8 | 25.9 | 39.5 | 58.8 |
| | | 48 | 4.5 | 3.8 | 2.8 | 2.1 | 11.8 | 25.3 | 37.3 | 55.3 |
| | | 240 | 3.1 | 1.5 | 1.2 | 0.7 | 8.1 | 10.1 | 15.6 | 17.2 |
| | | 480 | 0.4 | 0.3 | 0.2 | 0.2 | 1.1 | 2.0 | 3.0 | 4.2 |
| | | 720 | 0.3 | 0.2 | 0.2 | 0.1 | 0.9 | 1.4 | 2.0 | 2.9 |
| SD-W (a) | 3.8 | 48 | 14.5 | 9.6 | 7.0 | 5.0 | 38.3 | 63.2 | 92.1 | 132.9 |
| | | 240 | 14.5 | 9.3 | 6.6 | 4.8 | 38.3 | 61.3 | 87.1 | 127.5 |
| | | 480 | 13.4 | 8.6 | 6.1 | 4.4 | 35.3 | 56.7 | 80.6 | 115.6 |
| | | 720 | 8.3 | 4.0 | 3.4 | 2.4 | 22.0 | 26.0 | 45.1 | 63.8 |

Figures 3.1 through 3.8 establish the nominal flow capacity that each type of drain may sustain under variable hydraulic gradient and normal pressure conditions. These nominal (un-reduced) values will be used in selecting the appropriate type of drain for the given field conditions. Chapter 4 will discuss the methodology and results of seepage analysis which will establish the necessary drainage capacity of the aforementioned products for implementation in MSE structures.

## Chapter 4

## NUMERICAL ANALYSIS OF SEEPAGE

### 4.1 Slope Configuration

Several slope configurations were analyzed using the commercially available Finite Element Method (FEM) program Geo-Slope Office, Seep/W®. The objective of this analysis was to determine the phreatic surface and the rate of flow. The analyzed configurations provide a cross-section of slope layouts typically used in practice. By decreasing the steepness of the face batter (from vertical) it was possible to estimate the effects of a phreatic surface (emerging at various elevations) on the overall stability of the structure. The baseline model that is compatible with *American Association of State Highway and Transportation Officials (AASHTO)* design was developed with the following parameters: vertical slope height of 10m, geogrid reinforcement length of 7m (0.7H) and 0.4m vertical spacing and long term design strength, $T_{ltds}$ of 40kN/m, a segmental concrete block facing, cohesionless and homogeneous, reinforced and retained soil having permeability, $k = 8.64X10^{-2}$m/day, unit weight of, $\gamma = 20kN/m^3$ and internal angle of friction, $\phi = 30°$. Figure 4.1 illustrates the baseline model.

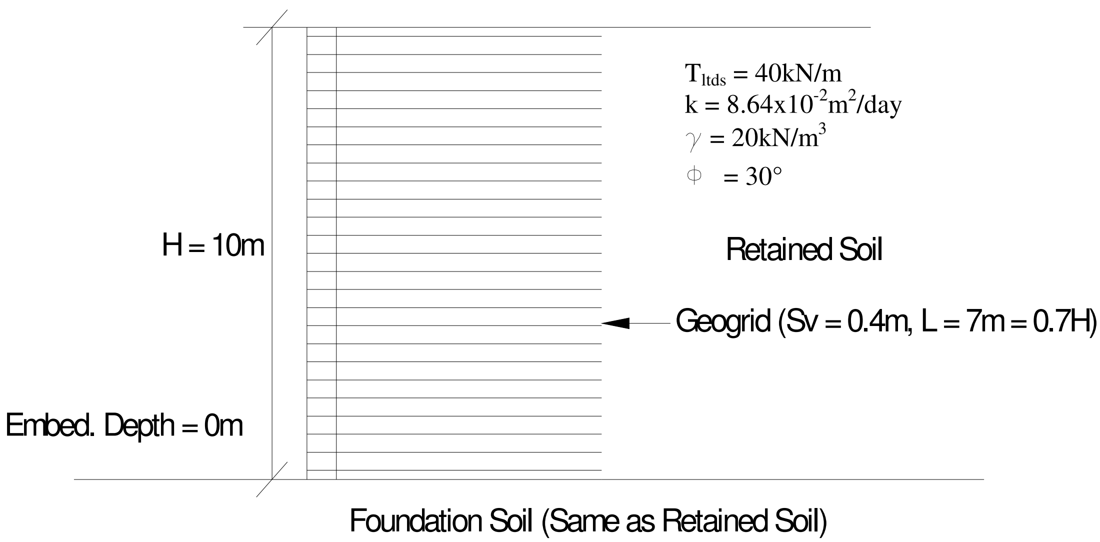


**Figure 4.1: Baseline Slope Configuration**
**Figure Not to Scale**

Two additional wall (or reinforced steep slope) configurations were analyzed one having a wall batter of 30° from vertical and the other 45° from vertical. Although the batter has a different geometry than the vertical slope the length, type and spacing of reinforcement, facing parameters and backfill soils remained the same as in the baseline model. Figures 4.2 and 4.3 represent the two additional wall configurations analyzed.

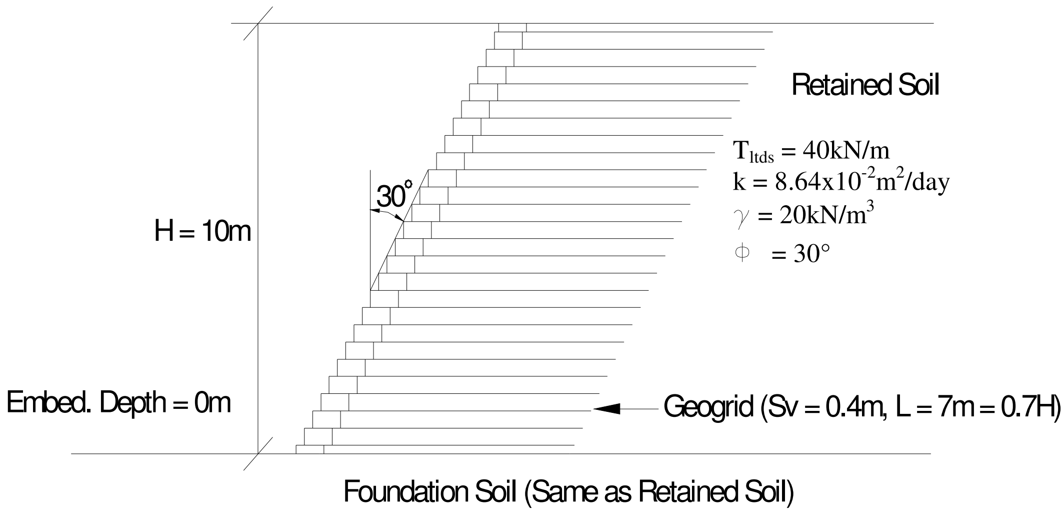


**Figure 4.2: 60° Slope Configuration**
**Figure Not to Scale**

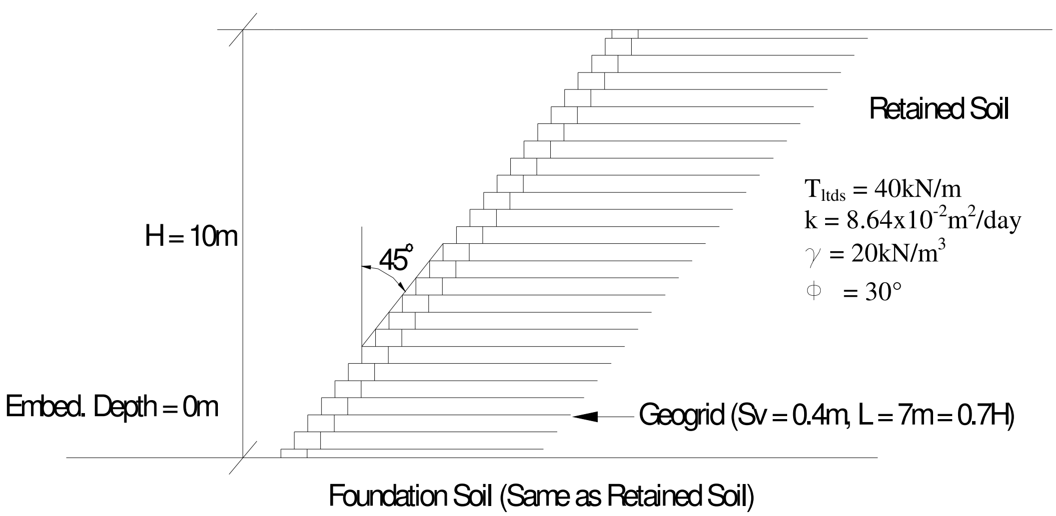


**Figure 4.3: 45° Slope Configuration**
**Figure Not to Scale**

## 4.2 Finite Element Analysis

The seepage analysis allowed determination of both the geometry of the phreatic surface and the resulting seepage rate that percolates through the reinforced soil zone.  Depending on what water head boundaries are specified the phreatic surface will emerge at various heights on the wall face.  The baseline configuration was initially analyzed with water head used as boundary conditions at 10m, prescribed at 20 m away from the face.  This case represents water at full height of the wall, up to 20m away from the wall; between that boundary and the drain, a phreatic surface develops as the water flows towards the drain.  When choosing the appropriate influence distance (i.e., the horizontal distance behind the wall face where the phreatic surface originates) special care was taken to ensure that negligible changes in the behavior of the phreatic surface resulted from variations in influence distance as explained next.

The FEM model was initially set up using a 10m by 20m area with a mesh spacing of 1m vertically and 2m horizontally.  The horizontal influence length was then increased to 40m which essentially yielded a lower phreatic surface line and hence less conservative results. An increase in mesh density showed no effects on results; hence, the selected mesh is satisfactory from a numerical standpoint.

For each wall configuration (shown in Figures 4.1 through 4.3) four separate analyses where run to model the effects of the phreatic surface originating from heights of 10m, 7.5m, 5m and 2.5m.   Each analysis utilized the predetermined influence distance of 20m behind the wall face with the mesh spacing set as described above.  Figure 4.4 illustrates a typical Seep/W graphical output that displays the mesh layout, flow discharge through the section and phreatic surface location for a 10m and head at the boundary. Each additional analysis yielded similar graphical representations from which flow discharge through the section and the geometry of the resulting phreatic surface may be determined.

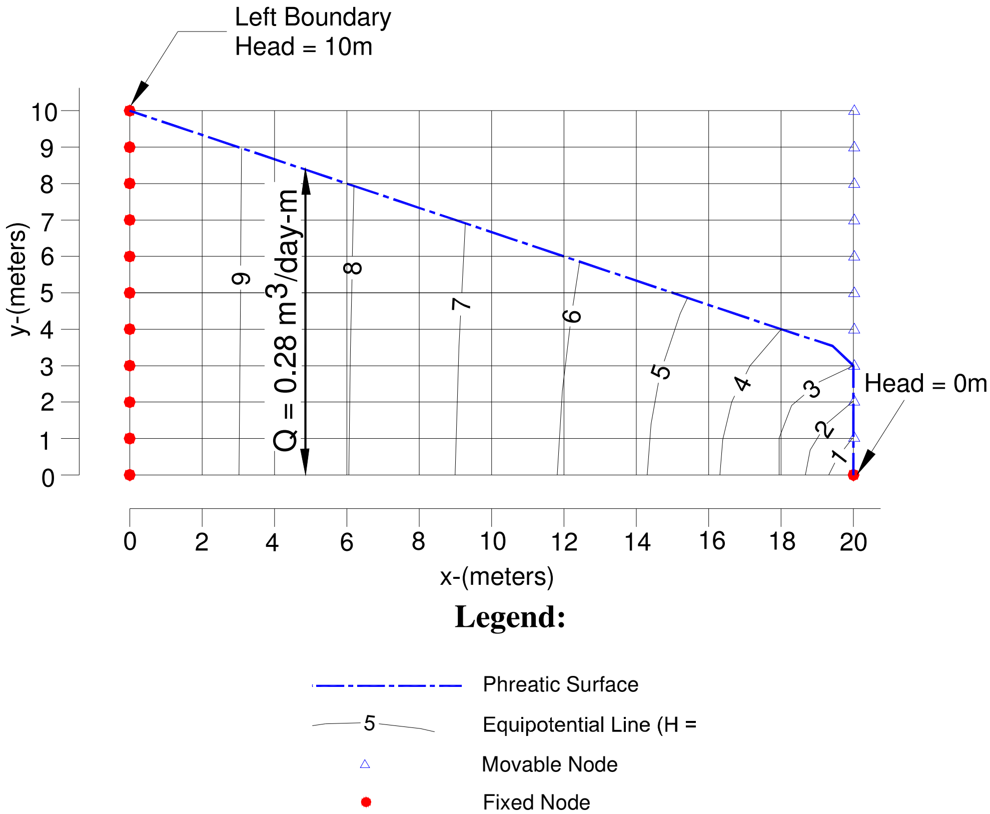


**Figure 4.4: Typical Seep/W Output: Phreatic Surface at 10m**

### 4.3 Drain Orientation

The geosynthetic drains are to be installed at the back face of the reinforced soil mass oriented parallel to the wall or slope face. Figure 4.5 illustrates the orientation of the drain relative to the wall or slope face.

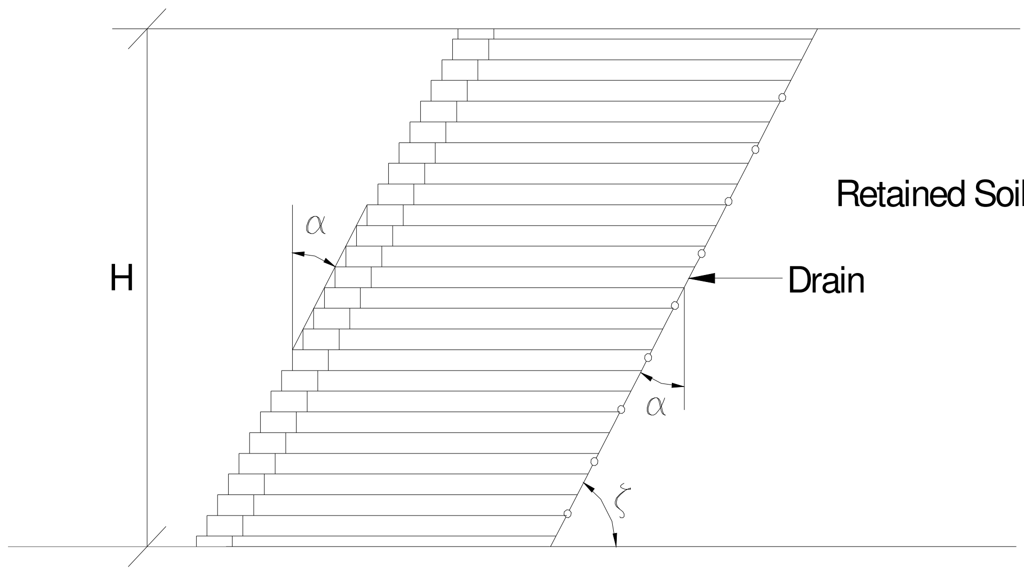


**Figure 4.5: Drain Orientation with respect to Face**
**Figure Not to Scale**

In Figure 4.5 the angle $\alpha$ represents the angle at which the wall or slope face is oriented with respect to vertical. The angle $\zeta$ represents the orientation of the drain with respect to horizontal. It can be shown that the hydraulic gradient, i, within the drain may be determined by using the basic property of a phreatic surface along which the pressure head is zero. By measuring the angle, $\zeta$, of the flow intercepting portion of the drain with respect to horizontal, one can obtain Equation 4 to determine the relevant value of i within the drain:

$$i = \sin \zeta \qquad (4)$$

Therefore, if the wall is inclined at an angle of 60° with respect to horizontal (i.e., $\zeta = 60°$) the resulting hydraulic gradient within the drain is defined as:

$$i = \sin(60°) = 0.866 \qquad (5)$$

**4.4 Results of Seepage Analysis**

The results of the seepage analysis were compiled in a similar manner as that of Figure 8 for each wall configuration. Table 4.1 provides a summary of the seepage results. The data found within Table 4.1 is based upon a soil permeability, $k = 8.64X10^{-2}$m/day, a 20m influence length and a 2m (horizontal) by 1m (vertical) mesh spacing. As stated in section 4.2, several additional runs were completed in which the permeability was both halved and doubled, the mesh spacing was made more dense and the influence length was increased to a maximum of 60m each of which yielded less conservative results and negligible changes in the output.

**Table 4.1: Summary of Seepage Results**

| **Hydraulic Gradient, i (in drain)*** | 1.0 | 0.866 | 0.707 |
|---|---|---|---|
| **Height of Water [m]** | **Flow Rate [$m^3$/day-m]** | | |
| 10 | 0.28 | 0.27 | 0.26 |
| 7.5 | 0.16 | 0.15 | 0.14 |
| 5 | 0.08 | 0.07 | 0.07 |
| 2.5 | 0.03 | 0.02 | 0.02 |

*as defined by discussion in section 4.3

Figures 4.6 through 4.9 provide a graphical format in which several wall configurations may be used to estimate the geometry of a phreatic surface for drain selection. The graphical representations from the Seep/W analysis were normalized in terms of wall height, y and horizontal influence distance, x relative to wall height.

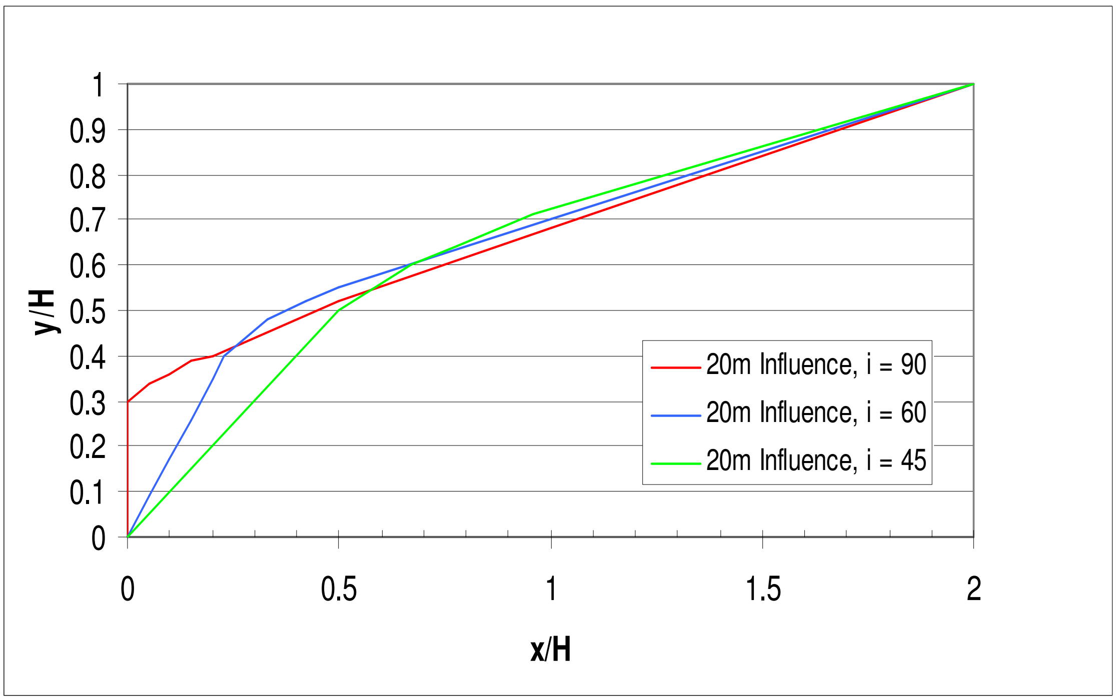


**Figure 4.6: Phreatic Surface $h_w/H = 1$**

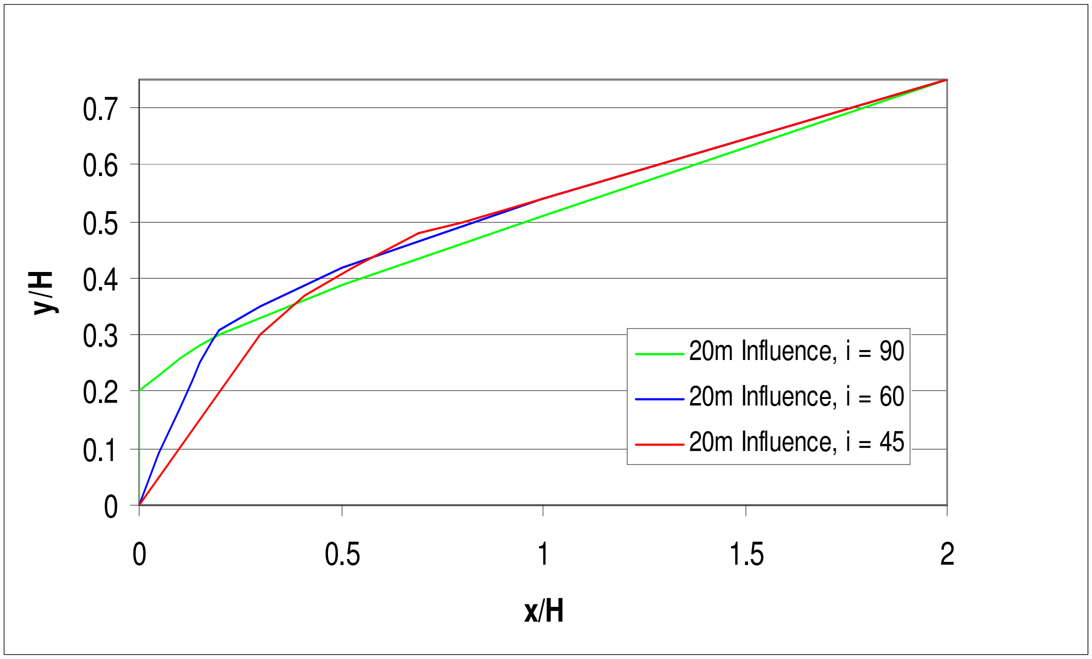


**Figure 4.7: Phreatic Surface $h_w/H = 0.75$**

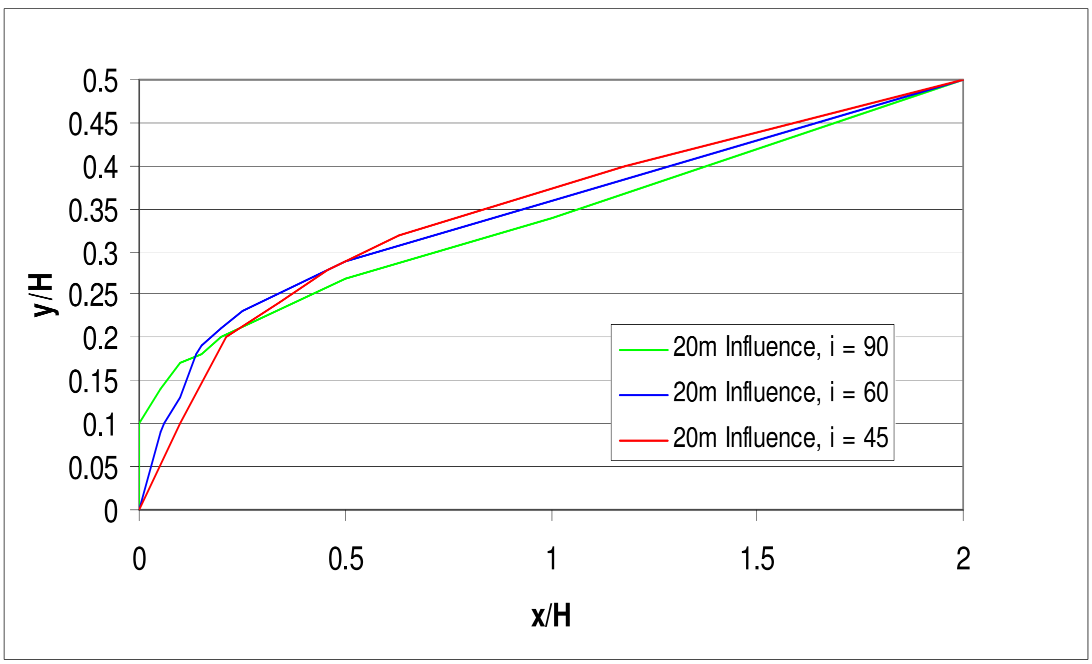


**Figure 4.8: Phreatic Surface $h_w/H = 0.5$**

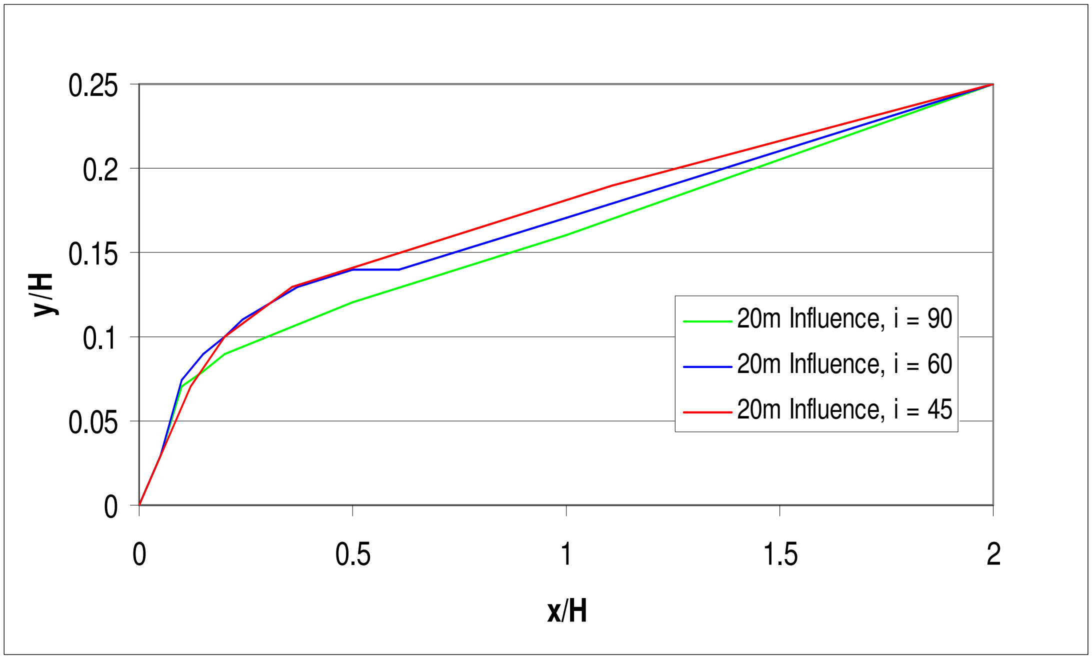


**Figure 4.9: Phreatic Surface $h_w/H = 0.25$**

Chapter 5 will discuss the implications set forth by the previous numerical analyses and provide parametric studies in which the wall geometry and phreatic surface parameters are varied to illustrate the advantages of implementing geosynthetic drains in MSE wall design.

# Chapter 5

# IMPLICATIONS OF NUMERICAL ANALYSIS: PARAMETRIC STUDIES

## 5.1 Stability Analysis Overview

With the aid of computer software nine parametric studies were completed which incorporate soil strength parameters, geosynthetic reinforcement properties, and influences of a phreatic surface to determine the overall effects of water on slope stability and the resulting Factor of Safety (FS) of geosynthetic reinforced earth structures. The data presented in Chapter 4, discussing the geometry of a phreatic surface seeping through the reinforced zone, was used to analyze several slope geometries both with and without the effects of water therefore establishing the importance and usefulness of implementing geosynthetic drains into MSE structures.

The computer program ReSSA® using a Bishop analysis procedure was used in this thesis where the target FS for global stability was set at 1.3 as prescribed in the AASHTO specifications (FHWA 2001). The software allowed for a drain to be installed directly behind the reinforced soil mass which essentially diverted the phreatic surface below and away from the reinforced soil. The soil strength parameters and hydraulic properties remained consistent with those discussed in Chapter 4 concerning the baseline wall properties. Table 5.1 summarizes the parametric studies conducted in this thesis.

**Table 5.1: Summary of Parametric Studies**

| Study No. | ζ* | Water Present in Reinforced Zone [ Yes or No] | Drain Installed [ Yes or No] | $H_w$** [m] |
|---|---|---|---|---|
| 1 | 90° | No | No | 10 |
| 2 | 90° | Yes | No | 10 |
| 3 | 90° | Yes | Yes | 10 |
| 4 | 60° | No | No | 10 |
| 5 | 60° | Yes | No | 10 |
| 6 | 60° | Yes | Yes | 10 |
| 7 | 45° | No | No | 10 |
| 8 | 45° | Yes | No | 10 |
| 9 | 45° | Yes | Yes | 10 |

*** wall or slope face inclination angle with respect to horizontal with drain oriented parallel to slope face (where applicable)**

**** phreatic surface origin height (as discussed in Chapter 4)**

## 5.2 Parametric Studies

*Study 1: Baseline Slope Configuration*

The first analysis considered the baseline slope without the effect of water within the reinforced soil zone. The wall geometry, reinforcement parameters and soil properites for the baseline slope are provided in Figure 5.1.

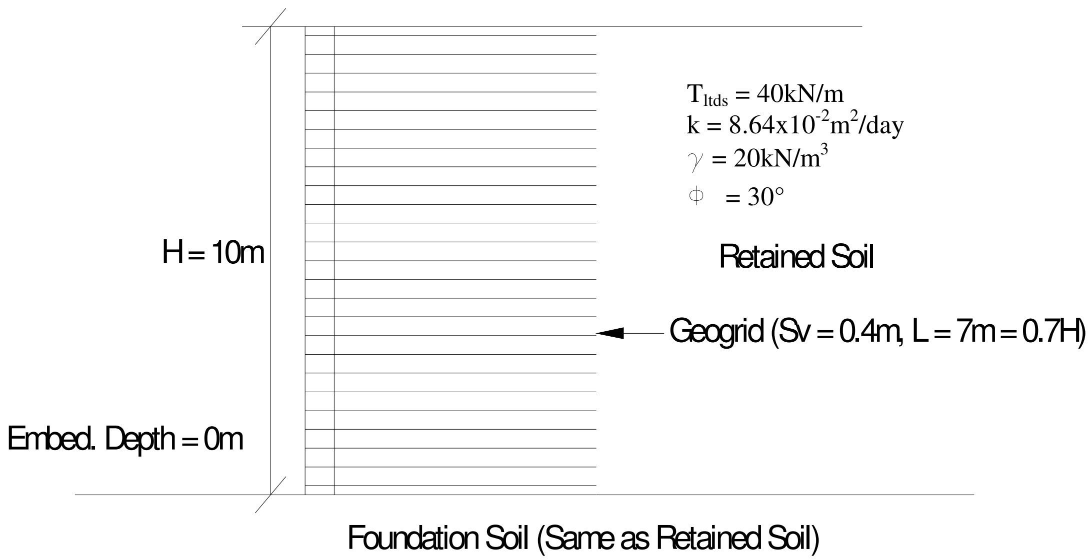


**Figure 5.1: Baseline Slope Configuration**
**Figure Not to Scale**

This initial analysis yielded a FS of 1.52 which exceeds the minimum value set forth by AASHTO. Figure 5.2 represents a safety map generated by the software. Notice that the entire region surrounding the critical slip surface exceeds the minimum FS value of 1.3.

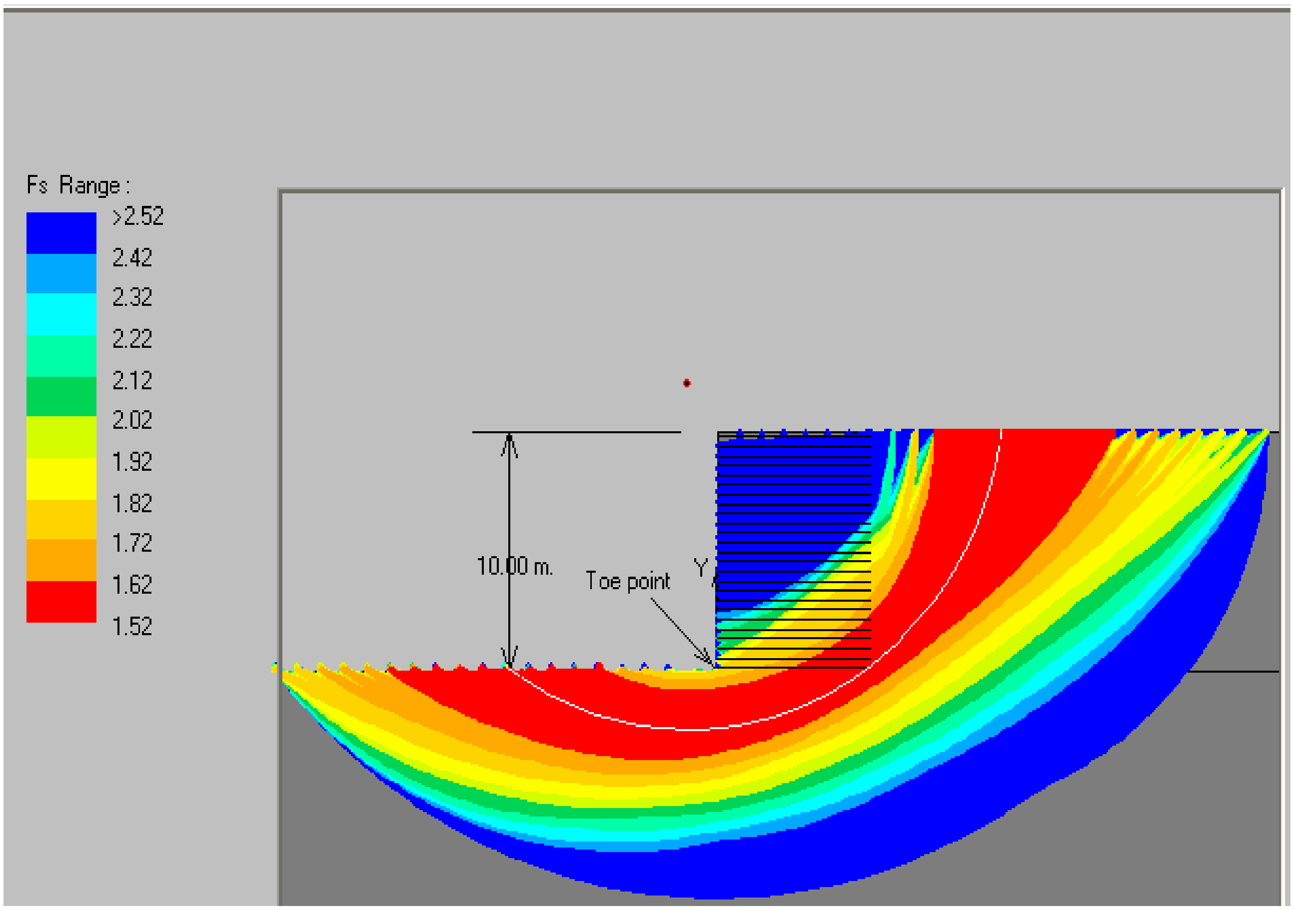


**Figure 5.2: Safety map under dry conditions**

*Study 2: Baseline Slope Configuration*

The second analysis was conducted to include the effect of water without the use of a drain. This study replicates the behavior of a reinforced soil structure with the presence of water in the reinforced soil mass. The phreatic surface shown in Figure 5.3 was extracted from Figure 4.6 found in Chapter 4. This run yielded a FS of 1.06. Figure 5.3 represents a safety map generated by the software. The entire red region indicates the portion of the wall section that is inadequate as the FS there is less than 1.3. Notice that the relative location of the critical slip surface has not moved when compared to that of Figure 5.2 indicating that the reinforced soil mass is of sufficient strength to prevent internal failure. However, deep seated failure is represented by a large soil zone.

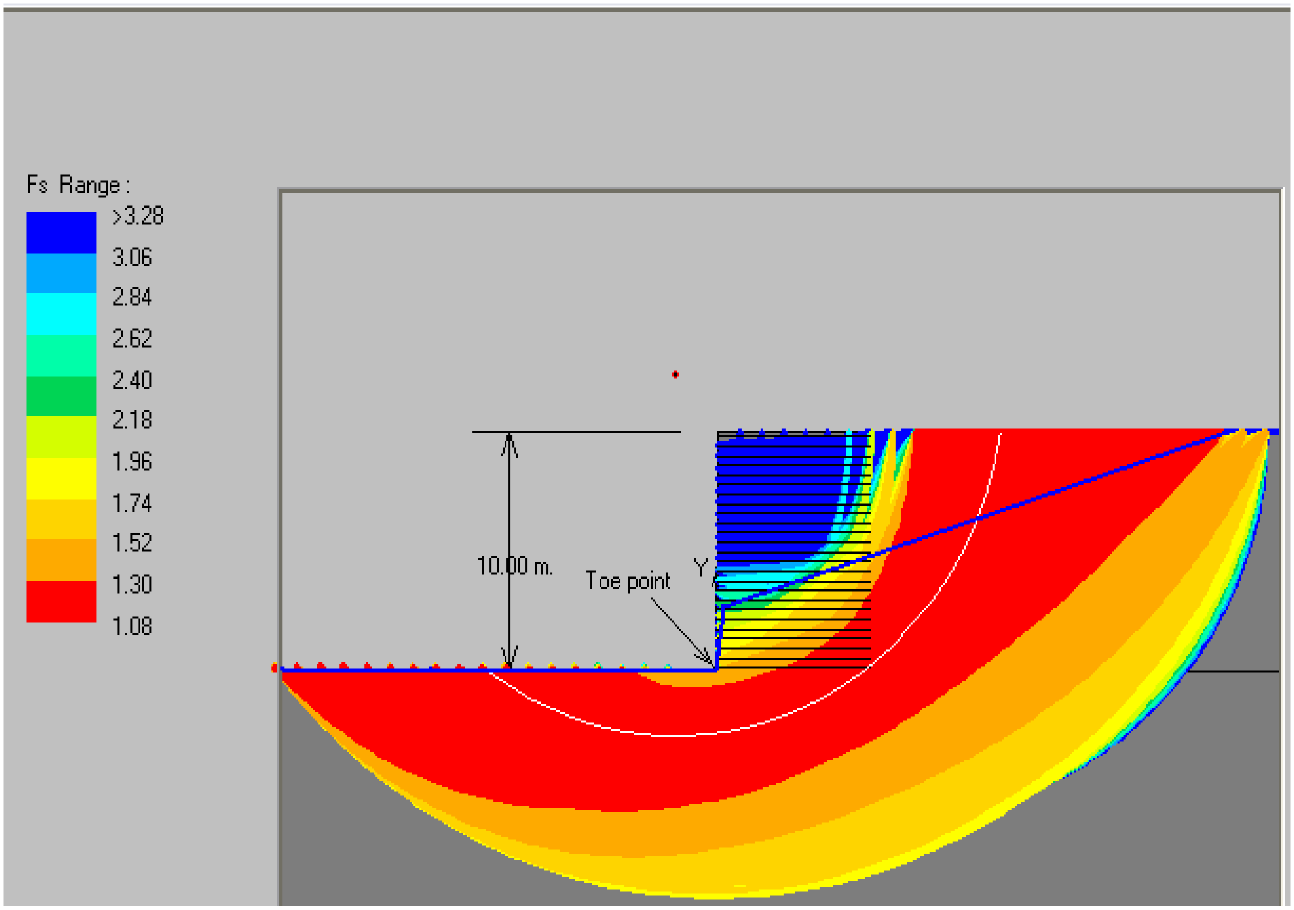


**Figure 5.3: Safety map with effect of water**

*Study 3: Baseline Slope Configuration with Drain*

To increase the effective shear strength of the soil along the critical slip surface and hence increase the FS in this region, a drain may be placed directly behind the reinforced soil zone to essentially intercept the phreatic surface and divert it below the reinforced soil zone (Leshchinsky 2005). Figure 5.4 provides a safety map with a drain installed. Notice that the FS increases to an acceptable value of $1.28 \approx 1.3$. Again, as in Figure 5.2, notice that the critical slip surface is positioned in the same location as in the initial analysis without the effects of water.

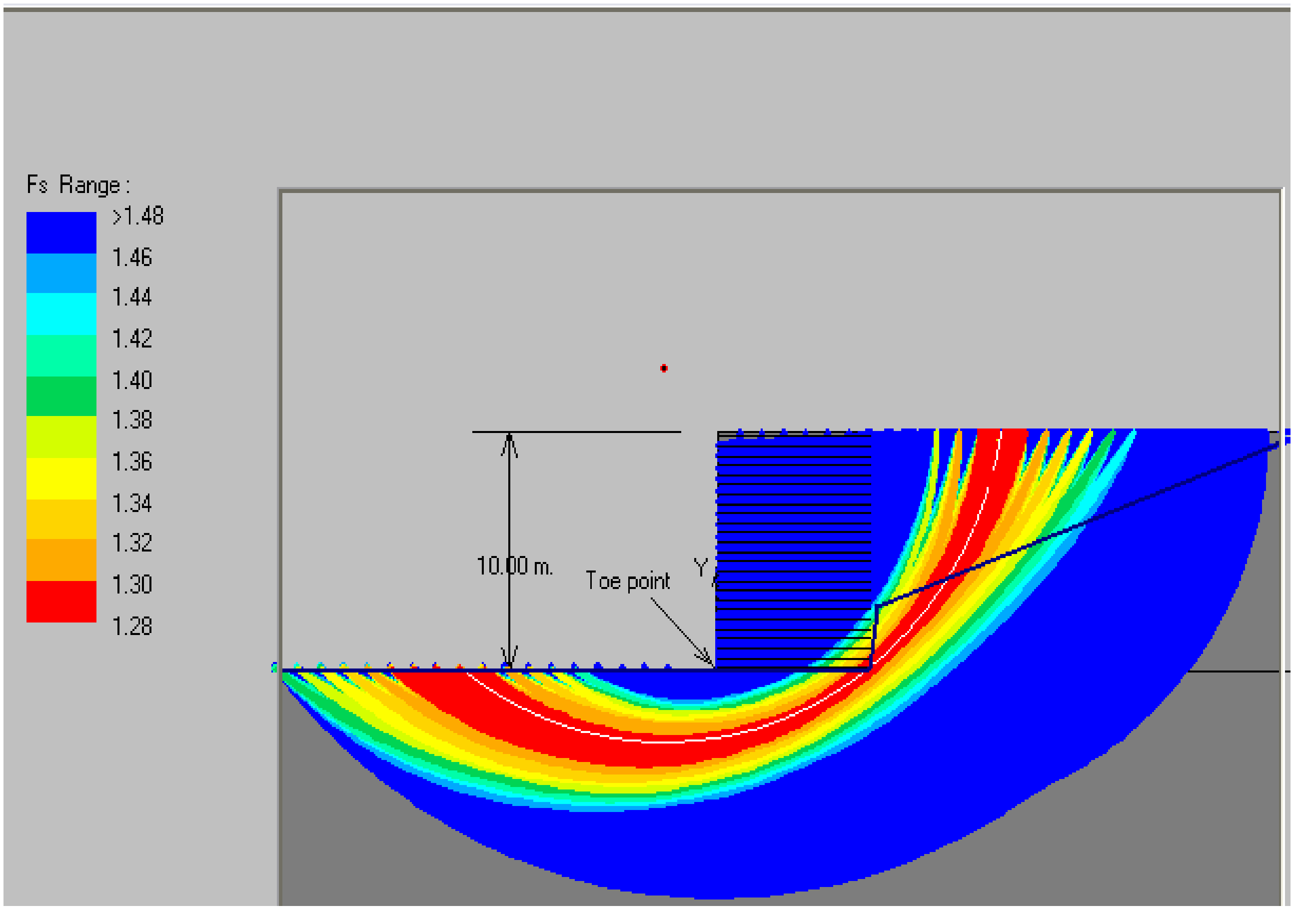


**Figure 5.4: Safety map with drain installed**

*Study 4: 60° Slope Configuration*

The fourth analysis considered the baseline slope with a 60° face inclination ($\zeta$ = 60°) without the effect of water within the reinforced soil zone. The wall geometry and reinforcement parameters for the baseline wall are provided in Figure 5.5.

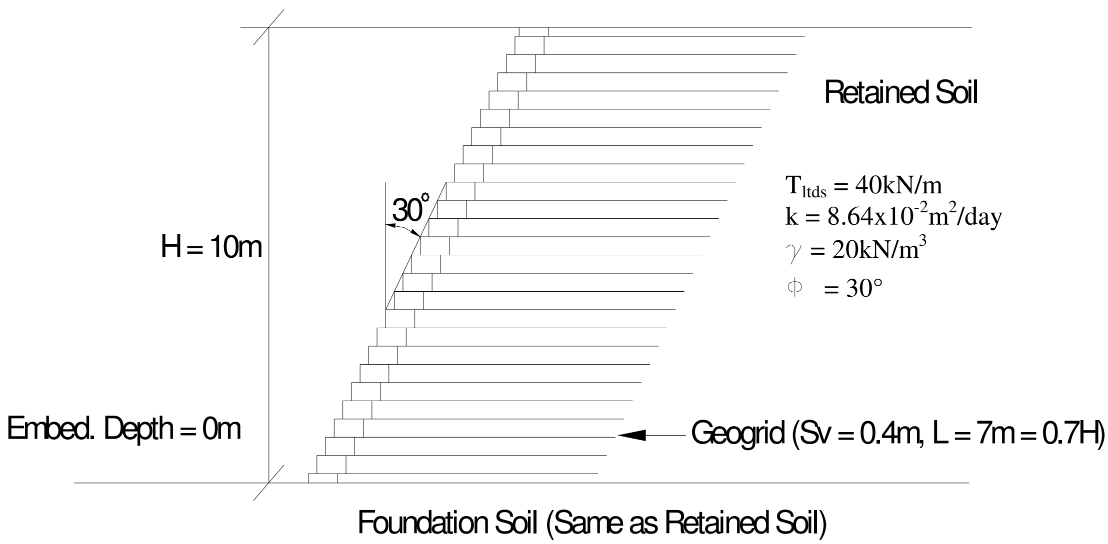


**Figure 5.5: 60° Slope**
**Figure Not to Scale**

This analysis yielded a FS of 1.39. Figure 5.6 represents the corresponding safety map generated by the software. Notice that the entire region surrounding the critical slip surface exceeds the minimum FS value of 1.3.

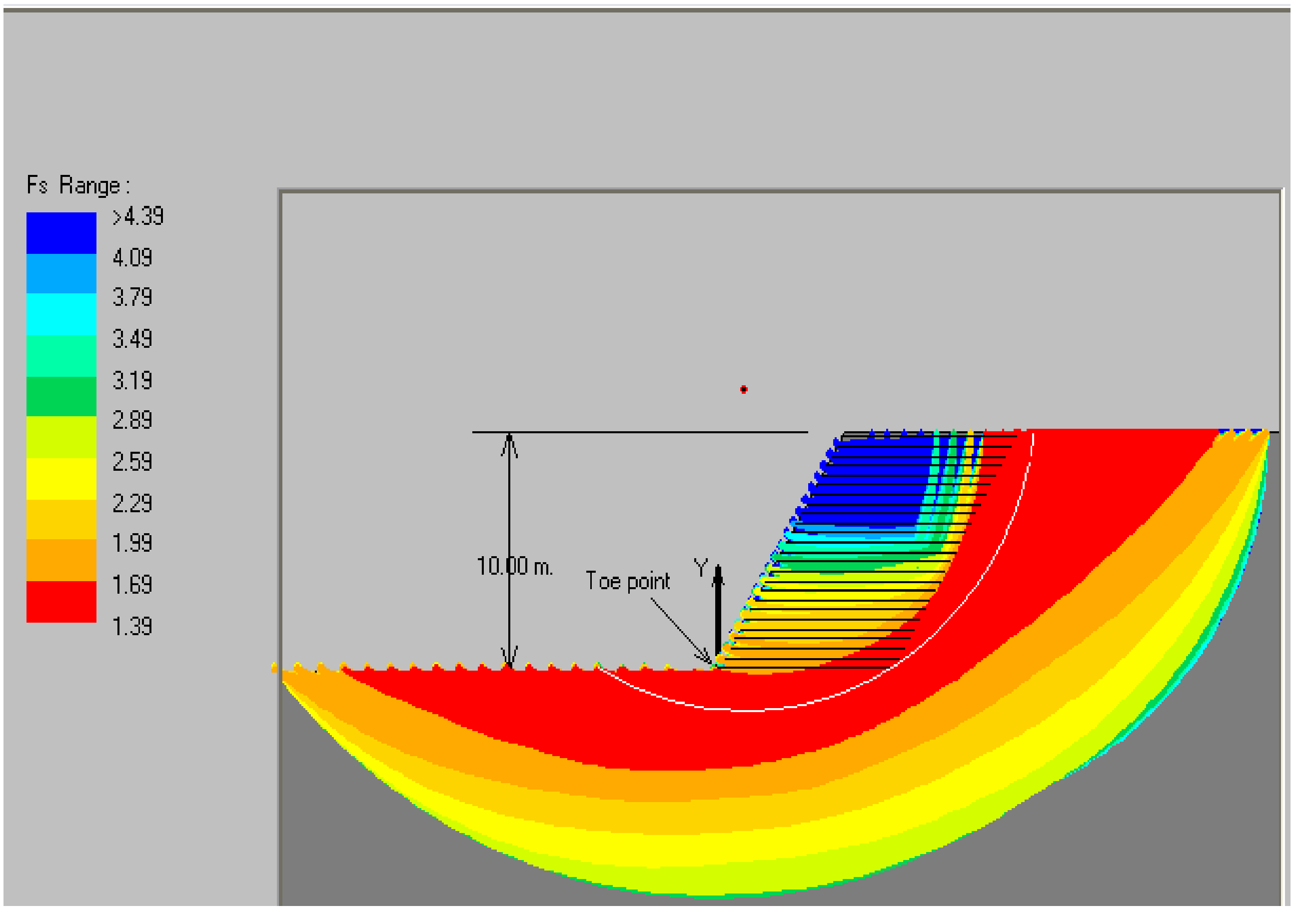


**Figure 5.6: Safety map for dry conditions**

*Study 5:  60° Slope Configuration*

In this analysis the effects of water are considered.  The phreatic surface shown in Figure 5.7 was extracted from Figure 4.6 found in Chapter 4.  This run yielded a FS of 0.93.  The entire red region indicates the portion of the wall section that is inadequate as the FS there is less than 1.3.

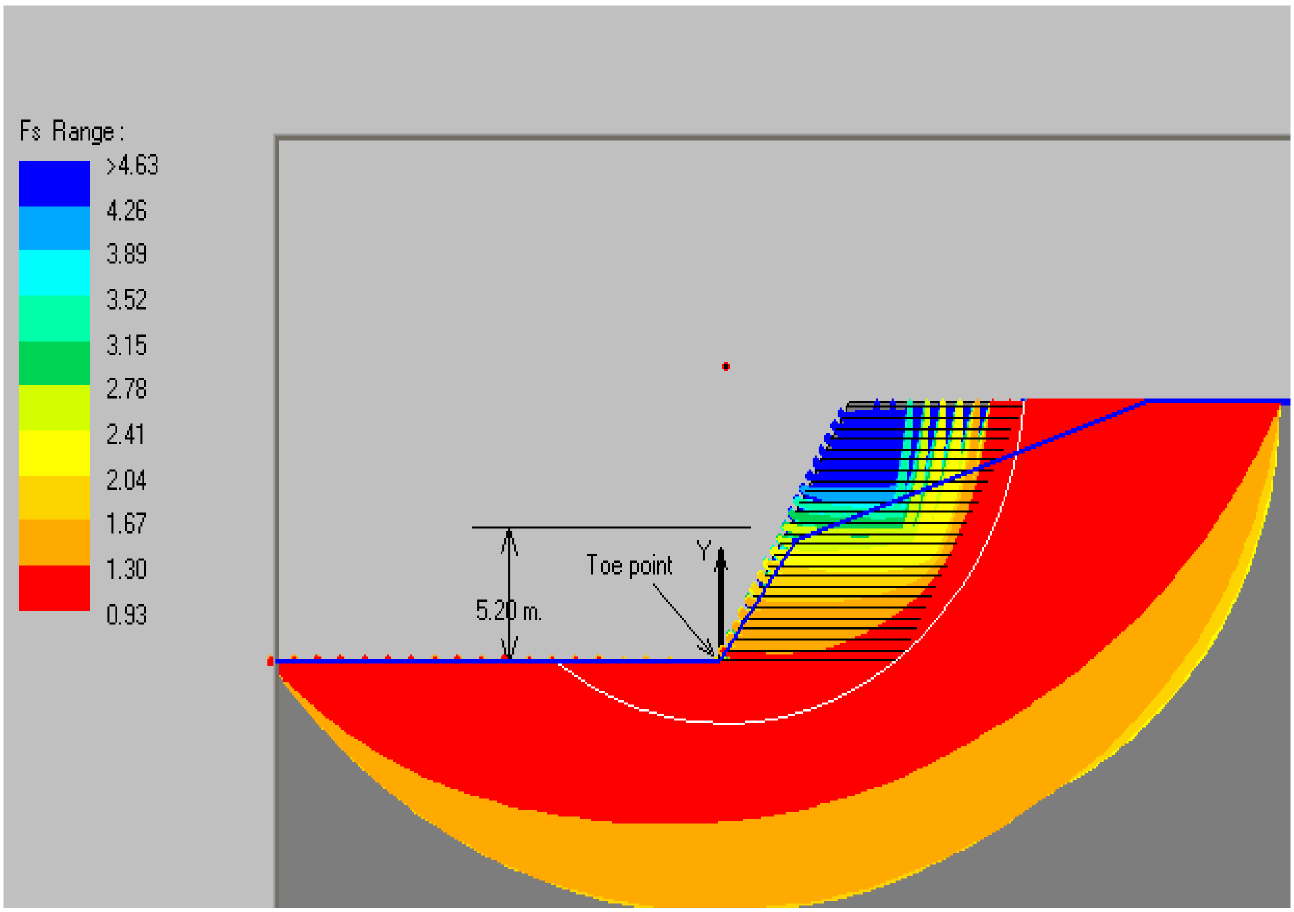


**Figure 5.7: Safety map with effect of water**

*Study 6:  60° Slope Configuration with Drain*

In order to increase the FS along the critical slip surface it was necessary to place a drain behind the reinforced zone as in Study 3.  In addition, the base layer of reinforcement was lengthened to 12m (1.2H) to increase the FS to 1.32.  Figure 5.8 provides a safety map with a drain installed behind the reinforced zone and a longer layer of basal reinforcement.  Notice that the critical slip surface is located in the same relative position as that in Figure 5.7.   The increased length of the base layer of reinforcement intercepts this slip surface and therefore raises the FS to an acceptable level.

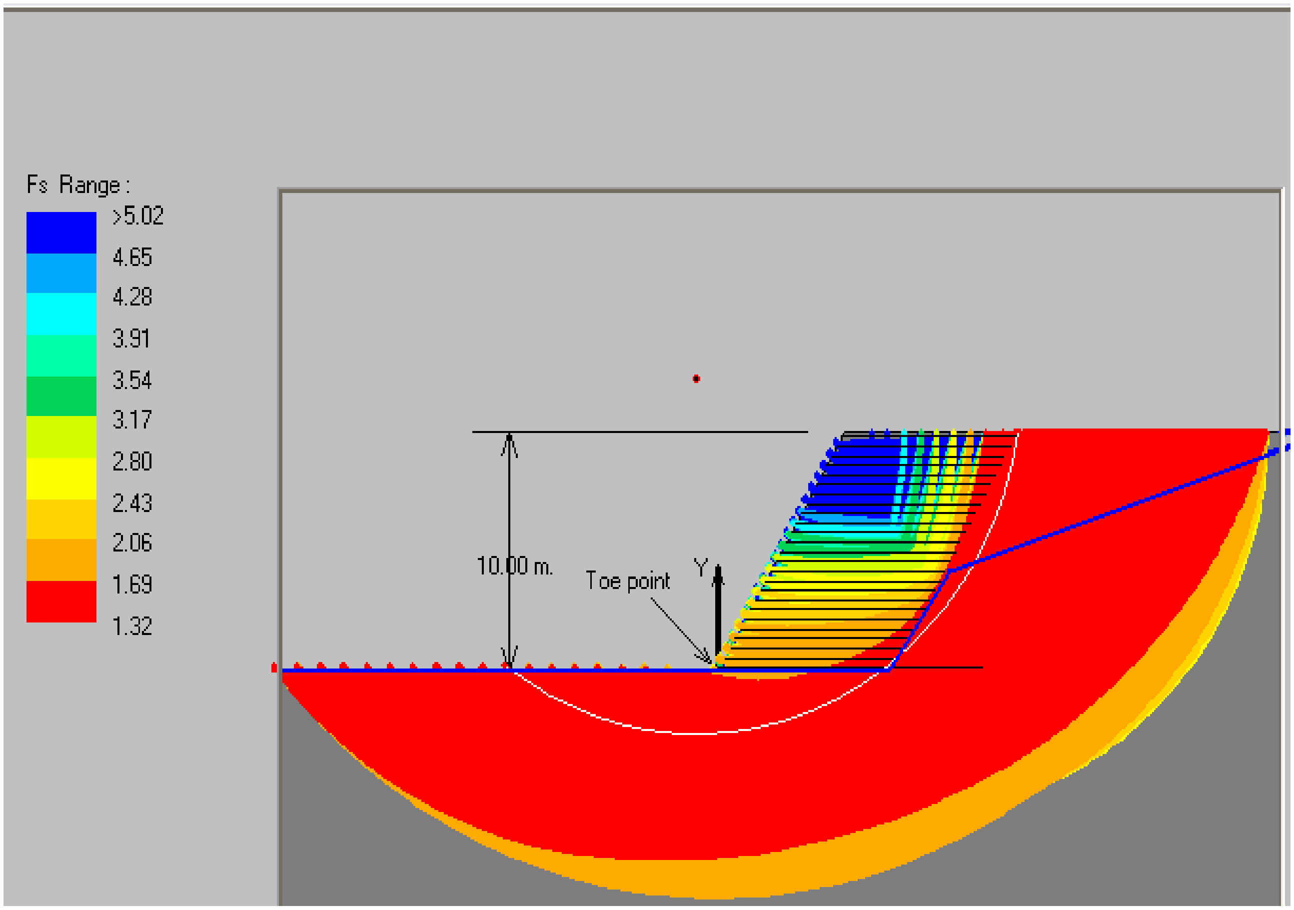


**Figure 5.8: Safety map with drain installed**

*Study 7: 45° Slope Configuration*

This analysis considers the baseline slope with a 45° face inclination ($\zeta = 45°$) without the effect of water within the reinforced soil zone. The wall geometry and reinforcement parameters for the baseline wall are provided in Figure 5.9.

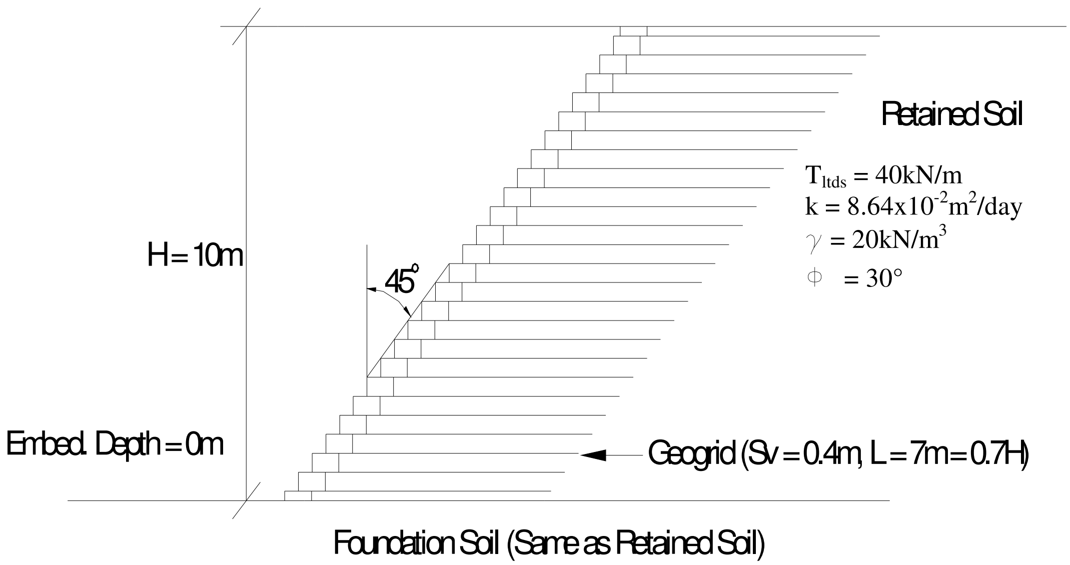


**Figure 5.9: 45° Slope**
**Figure Not to Scale**

Again the desired FS was lowered to 1.3 which is considered acceptable for deep seated failure according to the AASHTO specifications. This analysis yielded a FS of 1.32. Figure 5.10 represents the corresponding safety map generated by the software. Notice that the entire region surrounding the critical slip surface exceeds the minimum FS value of 1.3.

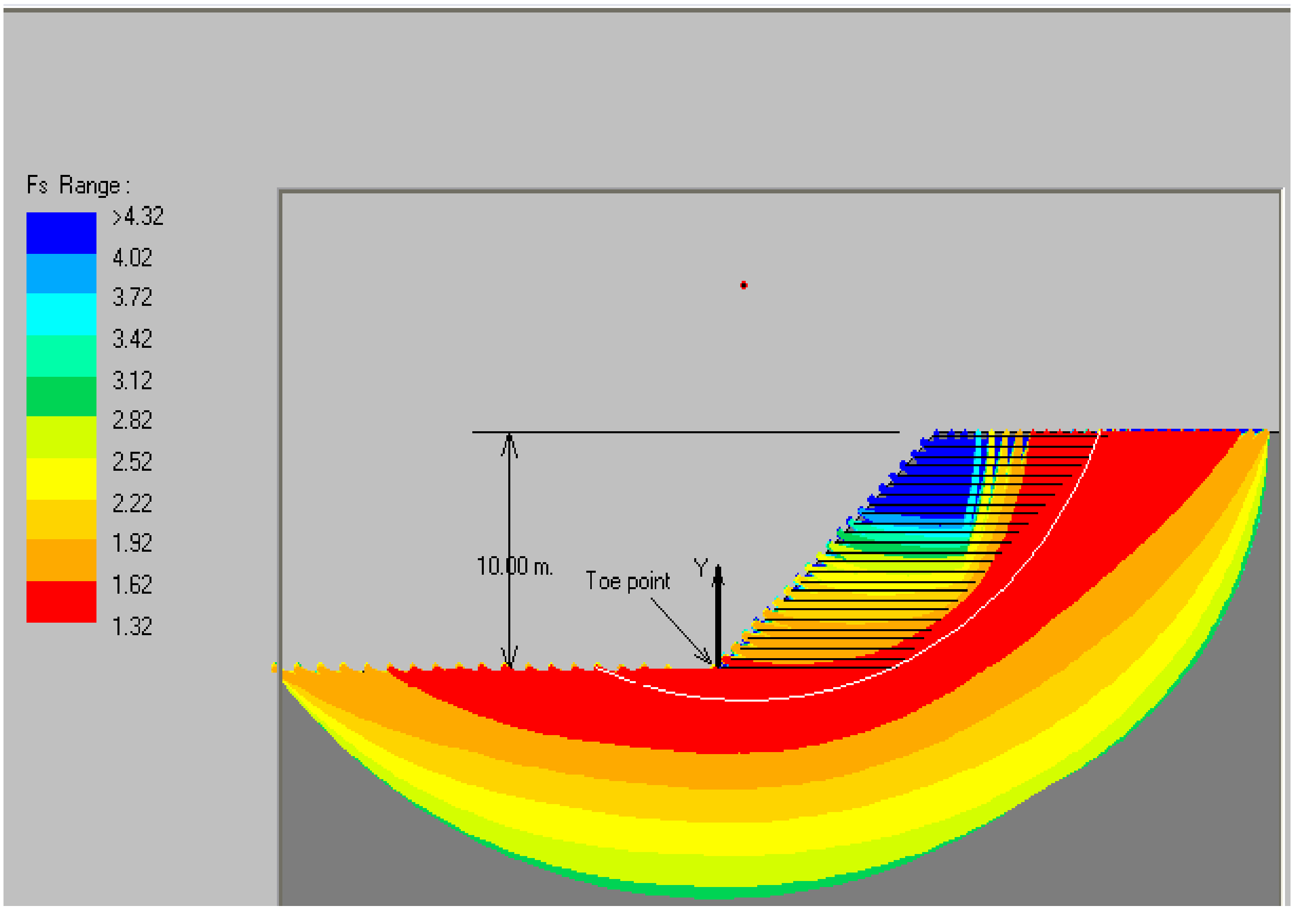


**Figure 5.10: Safety map for dry conditions**

*<u>Study 8:  45° Slope Configuration</u>*

In this analysis the effects of water are considered.  The phreatic surface shown in Figure 5.11 was extracted from Figure 4.6 found in Chapter 4.  This run yielded a FS of 0.93.  The entire red region indicates the portion of the wall section that is inadequate as the FS there is less than 1.3.

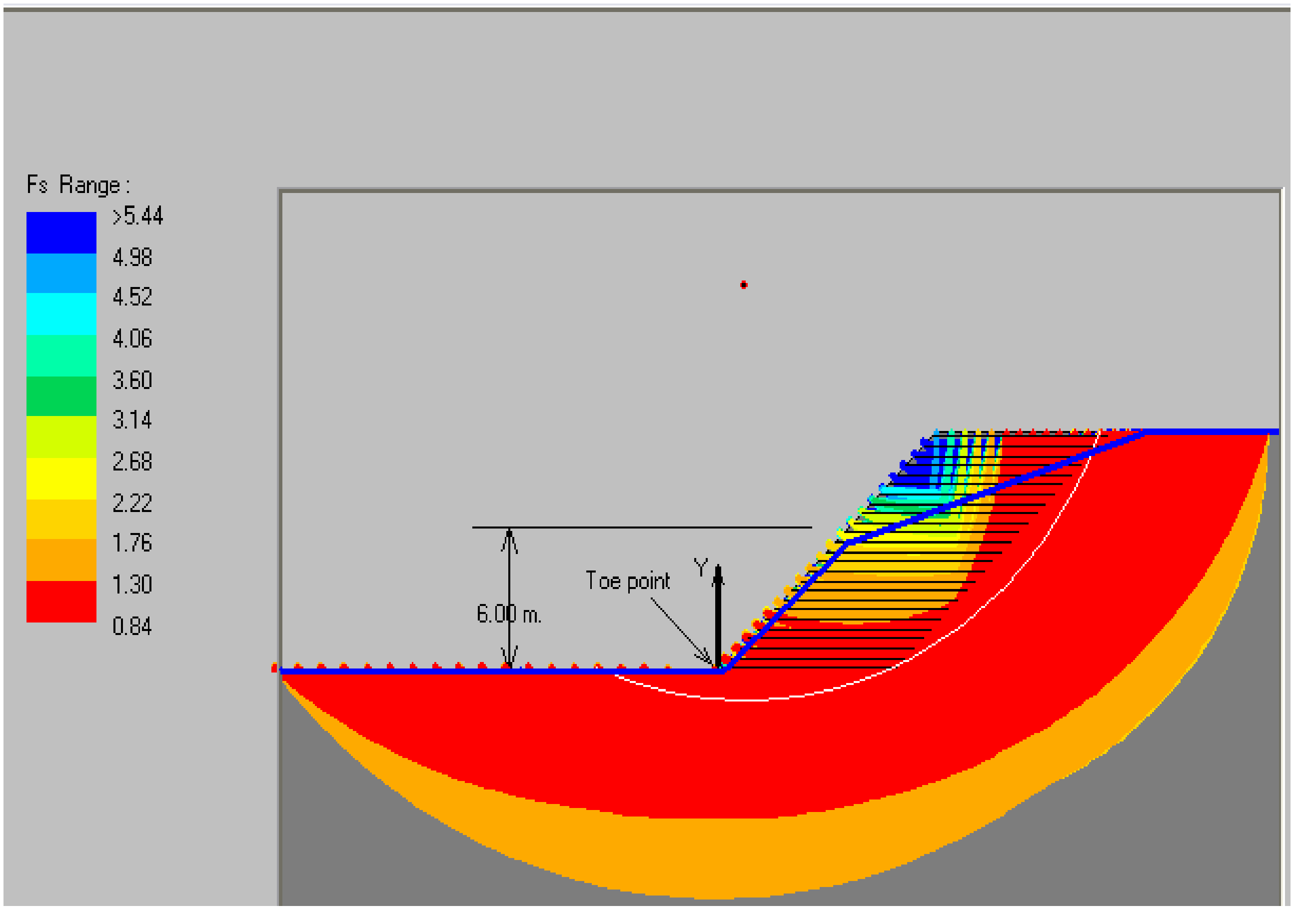


**Figure 5.11: Safety map with effect of water**

*Study 9: 45° Slope Configuration with Drain*

In order to increase the FS along the critical slip surface it was necessary to place a drain behind the reinforced zone as in Studies 3 and 6. Again, it was necessary to lengthen the base layer of reinforcement to 12m (1.2H) to increase the FS to 1.32. Figure 5.12 provides a safety map with a drain and longer layer of basal reinforcement. Notice that the critical slip surface has shifted deeper into the retained soil zone relative to its location in Figure 5.11.

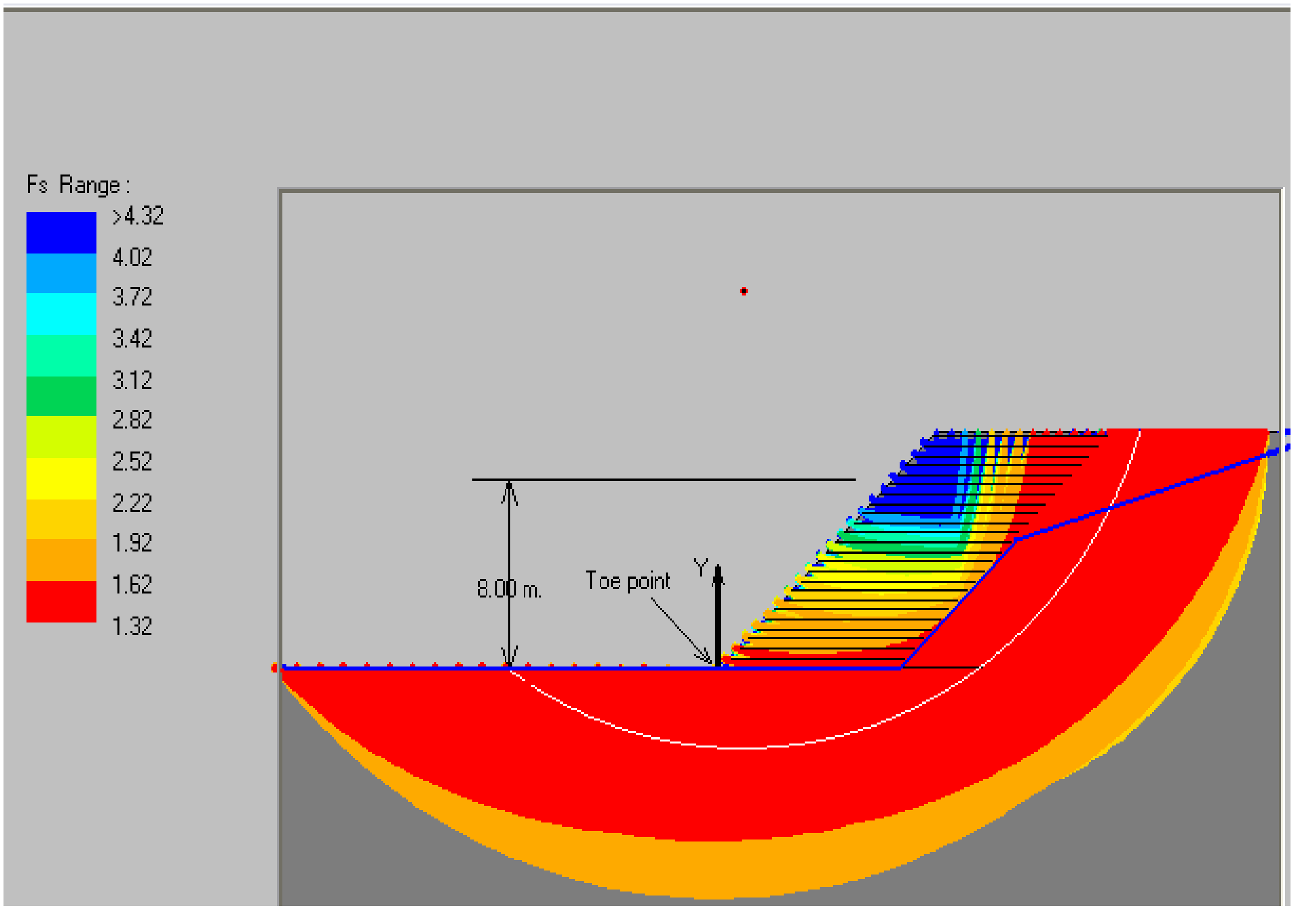


**Figure 5.12: Safety map with drain installed**

## 5.3 Implications

The parametric studies included in this section illustrate the effectiveness of utilizing the geosynthetic drains (discussed in Chapter 2) in conjunction with slight variations in reinforcement properties in a generic manner to increase the FS to acceptable values where water is present in the reinforced soil zone. The aforementioned parametric studies provide the following implications: a) the presence of water in the reinforced soil zone decreases stability; shifting the location of the phreatic surface behind the reinforced zone by utilizing a drain increases stability to acceptable values as per AASHTO guidelines; b) if no drain is used, to achieve a certain stability longer and stronger reinforcement is needed; the cost of properly selected drain is typically cheaper than the extra reinforcement and the labor associated with placement of reinforcement and its backfill; c) it is clear that the reinforcement used is probably stronger than needed for global stability as the critical zone is pushed back to the rear of the reinforcement; a little weaker reinforcement where internal failures give FS = 1.5 will work for global stability but might not be suitable based on lateral earth pressures as dictated by AASHTO.

Chapter 6 will outline two example problems where a particular drain is chosen to act as a drain material and respective reduction factors are applied to its nominal (measured) flow capacity to introduce conservatism into the drain selection procedure to account for reduction factors not measured in the experimental portion of this thesis.

Chapter 6

# INTEGRATION OF SLOPE STABILITY ANALYSIS, SEEPAGE ANALYSIS AND EXPERIMENTAL APPROACH IN DESIGN

The purpose of this chapter is to provide two representative example problems which illustrate the drain selection procedure to accommodate variable slope geometries. The process will incorporate the experimental data discussed in Chapters 2 and 3, the seepage analysis discussed in Chapter 4, and the stability analyses conducted in Chapter 5.

## 6.1 General Drain Selection Procedure

The following five steps provide a guideline to selecting the proper drain to be installed to adequately drain the reinforced soil zone.

*Step One: Determine the Required Flow Capacity:*

The required flow capacity may be obtained from the FEM analysis generated by a program such as Seep/W® as shown in Table 4.1 in Chapter 4. Alternatively, construction of a proper flow net would yield the necessary data.

*Step Two: Determine maximum vertical stress drain will experience:*

In order to determine the maximum depth to which a drain may be installed one must make a conservative assumption in that the drain will be placed in a horizontal orientation in which the maximum vertical stress is defined by Equation 6:

$$\sigma \approx \gamma z \qquad (6)$$

where: $\sigma$ = the vertical stress at the point of concern
$\gamma$ = the soil unit weight
$z$ = the vertical depth to the point of concern

*Step Three: Determination of Drain Orientation:*

As discussed in Chapter 4 section 4.3, the drain shall be oriented parallel to the wall or slope face. Consequently, the following equation defines the hydraulic gradient within the drain:

$$i = \sin \zeta \qquad (7)$$

where: $\zeta$ = is the angle (in degrees) between the drain and horizontal the horizontal datum

*Step Four: Applying Reduction Factors*

A trial drain type may be chosen based on the experimental data (From Table 3.2 in Chapter 3) that fits both the hydraulic gradient, i, from Step 3 and the vertical stress value from Step 2. The nominal or experimental flow capacity (From Table 3.2 in Chapter 3) must be reduced following, for example, the guidance in Koerner and Koerner (2005) by applying appropriate reduction factors to account for factors that will likely hinder the drain's ability to uphold its nominal flow capacity during the life of the structure. Equation 8 defines the allowable flow capacity that is recommended for any geosynthetic used as a drainage medium and applies a suitable Factor of Safety to the experimental flow capacity:

$$q_{allaw} = q_{ult}\left[\frac{1}{RF_{in} \times RF_{cr} \times RF_{cc} \times RF_{bc}}\right] \quad (8)$$

where: $q_{allow}$ = allowable or design flow rate
$q_{ult}$ = measured or ultimate flow rate
$RF_{in}$ = reduction factor for the intrusion of geotextiles or geomembranes into the core of the drainage product
$RF_{cr}$ = reduction factor for creep of the drainage core or covering geosynthetics
$RF_{cc}$ = reduction factor for chemical clogging of the drainage core
$RF_{bc}$ = reduction factor for biological clogging of the drainage core

A typical range of reduction factors are (Koerner and Koerner (2005)):

**Table 6.1: Reduction Factors**

| Reduction Factor | Suggested Value |
|---|---|
| $RF_{in}$ | 1.3 to 1.5 |
| $RF_{cr}$ | 1.2 to 1.4 |
| $RF_{cc}$ | 1.1 to 1.5 |
| $RF_{bc}$ | 1.0 to 1.5 |

If in fact the reduced flow capacity, $q_{allow}$ (from Equation 8) of the trial drain exceeds the required flow capacity (from Table 4.1) then this particular drain is adequate. Otherwise, a drain with a higher flow capacity must be selected.

*Step Five: Check Stability*

In order to ensure that the drain selection adequately satisfies stability requirements it is necessary to run a stability analysis using the aforementioned program ReSSA® or any other comparable slope stability analysis program. Stability analyses shall be run both with and without the drain to establish the overall effectiveness of the drain and ensure that the structure will be stable.

### 6.2 Example Problem One

The first example problem requires selection of a drain for a geosynthetic reinforced structure having the following properties: vertical height of 10m, geogrid reinforcement length of 7m and 0.4m vertical spacing and long term design strength, $T_{ltds}$, of 40kN/m, a segmental concrete block facing, cohesionless and homogeneous, reinforced and retained soil having permeability, $k = 8.64X10^{-2}$m/day, unit weight of, $\gamma = 20kN/m^3$ and internal angle of friction, $\phi = 30°$. The water table is located at a height of 10m and is indicated by the blue line. Figure 6.1 illustrates the geometry of the wall section.

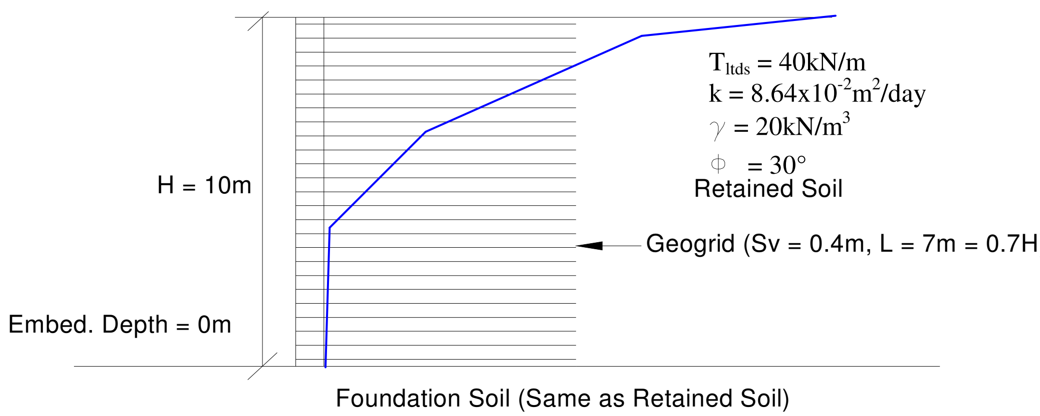


**Figure 6.1: Wall Geometry for Example 1**
**Figure Not to Scale**

**Solution:**

*Step One: Determining the Required Flow Capacity:*

Recall from Table 4.1 in Chapter 4 the following:

**Summary of Seepage Results**

| **Hydraulic Gradient, i (in drain)*** | 1.0 | 0.866 | 0.707 |
|---|---|---|---|
| **Height of Water [m]** | **Flow Rate [$m^3$/day-m]** | | |
| 10 | 0.28 | 0.27 | 0.26 |
| 7.5 | 0.16 | 0.15 | 0.14 |
| 5 | 0.08 | 0.07 | 0.07 |
| 2.5 | 0.03 | 0.02 | 0.02 |

*as defined by discussion in Chapter 4, section 4.3

The vertical wall height is 10m with its face oriented at 90° [$i_{drain} = \sin(90°) = 1.0$] with respect to horizontal therefore the required flow rate is **0.28 $m^3$/day-m**. Recall that the flow rate was established in a general fashion in Chapter 4 based on a flow net determined using finite element analyses. However, such an analysis is not needed for simple cases as the runs in this work have established a procedure to estimate the rate of flow using normalized results.

*Step Two: Determine maximum vertical stress drain will experience:*

The maximum vertical stress the drain will experience is:

$$\sigma \approx \gamma z = (20\text{kN/m}^3)(10\text{m}) = \mathbf{200kPa}$$

*Step Three: Determination of Drain Orientation:*

The hydraulic gradient within the drain is:

$$i = \sin \zeta = (\sin 90°) = \mathbf{1.0}$$

*Step Four: Applying Reduction Factors*

From Table 3.2 in Chapter 3 a GT-NW (a) non-woven geotextile is chosen as a trial drain. At a hydraulic gradient of 1.0 and normal stress of 240kPa this drain accommodates a flow rate of **0.44 m$^3$/day-m**. Applying the relevant reduction factors yields:

$$q_{allaw} = q_{ult}\left[\frac{1}{RF_{in} \times RF_{cr} \times RF_{cc} \times RF_{bc}}\right] = 0.44\left[\frac{1}{(1.4)(1.3)(1.3)(1.3)}\right] = \mathbf{0.14m^3/day - m}$$

Because **0.14 m$^3$/day-m < 0.28 m$^3$/day-m** the trail drain selection is not adequate. Returning to Table 3.2 in Chapter 3 a GC(a) geo-composite is chosen as a second trial drain. At a hydraulic gradient of 1.0 and normal stress of 240kPa this drain accommodates a flow rate of **2.4 m$^3$/day-m**. Again, applying the relevant reduction factors:

$$q_{allaw} = q_{ult}\left[\frac{1}{RF_{in} \times RF_{cr} \times RF_{cc} \times RF_{bc}}\right] = 2.4\left[\frac{1}{(1.4)(1.3)(1.3)(1.3)}\right] = \mathbf{0.78m^3/day - m}$$

Because **0.78 m$^3$/day-m > 0.28 m$^3$/day-m** the second trail drain selection is adequate.

*Step Five: Check Stability*

Figure 6.2 is a safety map generated from ReSSA without a drain installed (i.e., water is present within the reinforced soil zone). The minimum FS indicated by the red region is 1.08 and is considered inadequate as per AASHTO guidelines.

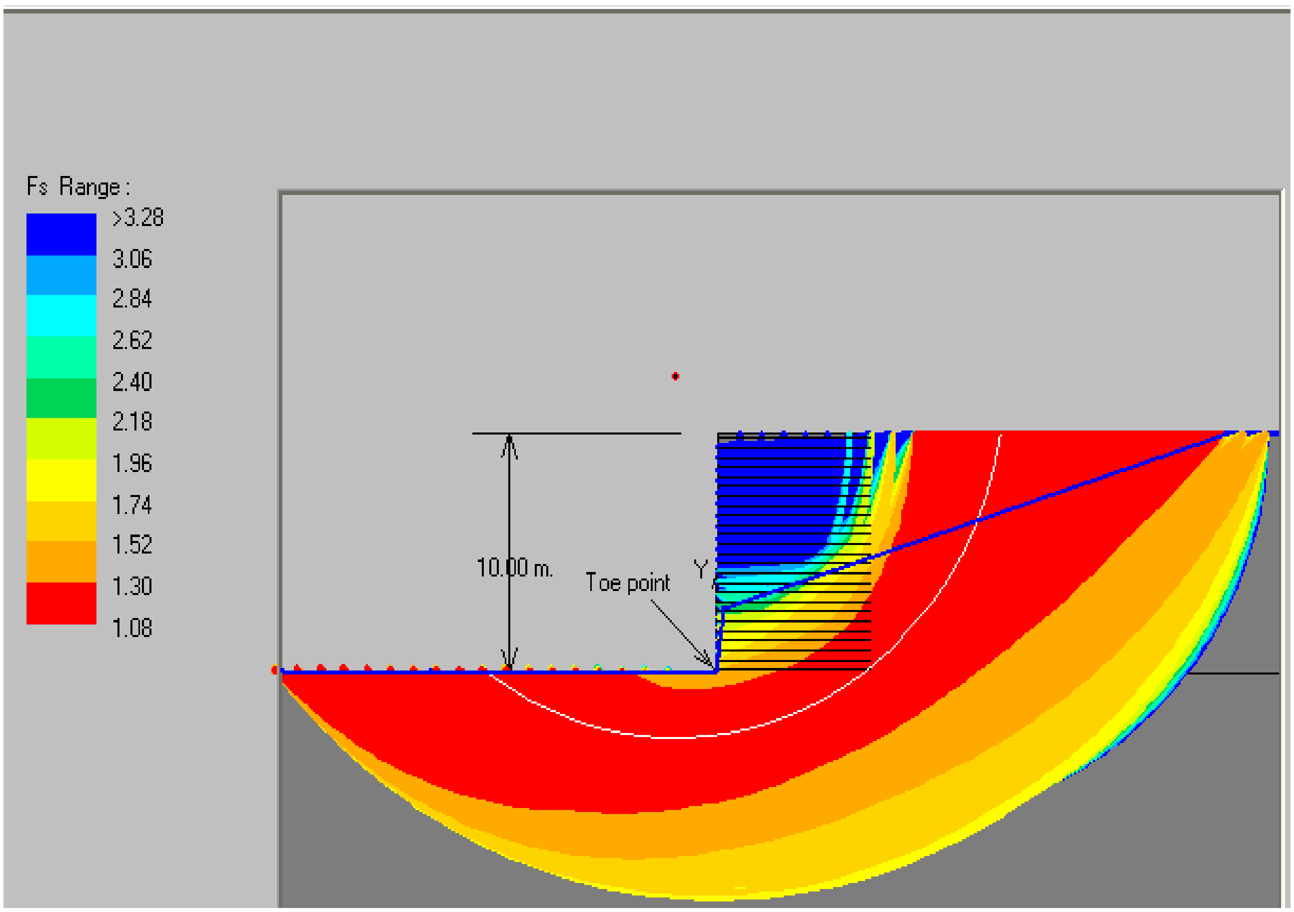


**Figure 6.2: Safety map with effect of water**

An additional stability analysis was run illustrated by Figure 6.3 with a drain installed which essentially drains the reinforced soil zone.  Notice that in this case the FS was raised to 1.28 ≈ 1.3 and is considered adequate as per AASHTO guidelines.

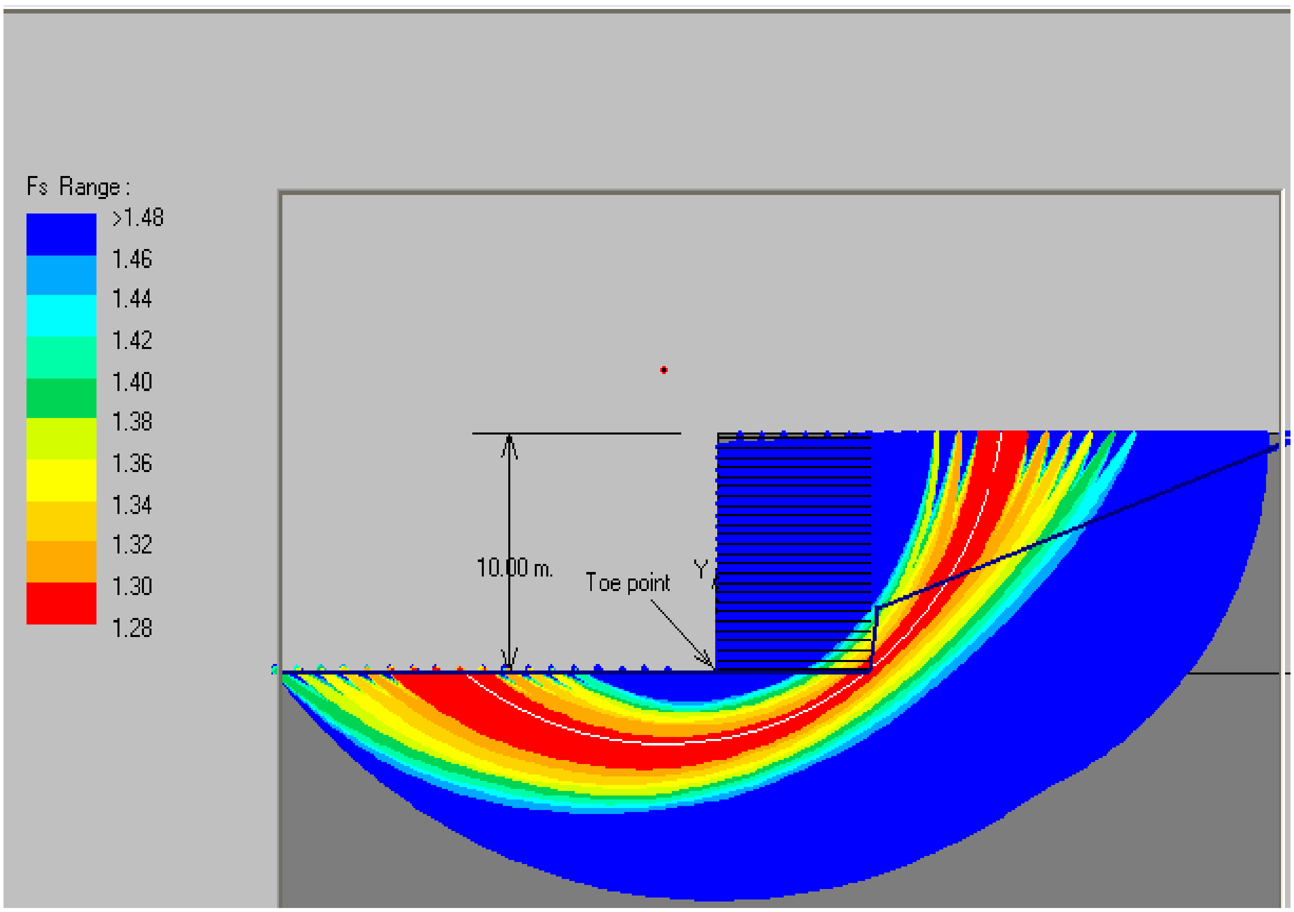


**Figure 6.3: Safety map with drain installed**

### 6.2.1 Drain Installation

Several alternatives exist as to how the drain may be installed to adequately drain the reinforced soil zone. Figures 6.4 and 6.5 illustrate two common layouts which may be implemented at the discretion of the wall designer and contractor. Each method is considered adequate however material availability and experience of the installer will dictate which method is considered the most desirable solution.

Figure 6.4 illustrates the use of the geosynthetic drain installed parallel to the wall face with a pipe placed parallel to the wall face to intercept water flow from the drain and lateral pipe outlets which transfers the water from the pipe behind the reinforced soil zone to the toe of the wall. The pipe should be installed at a grade that allows the flow of water and while daylighting beyond the footing of the wall.

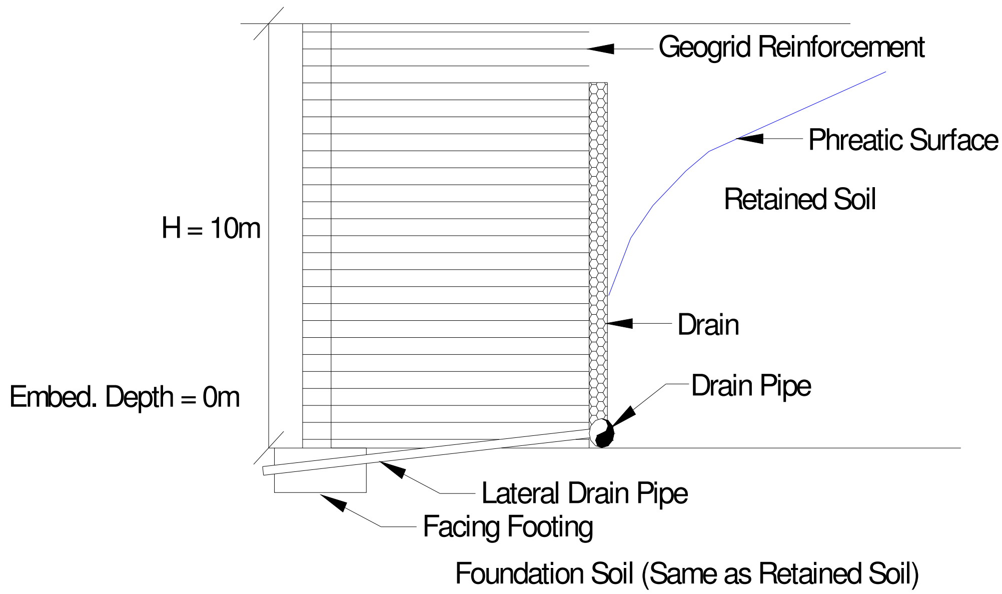


**Figure 6.4: Drain Installation Schematic**
**Figure Not to Scale**

Alternatively, the network of pipes may be replaced by a granular base material which transfers the water from the drain to the toe of the wall. Figure 6.5 illustrates this layout.

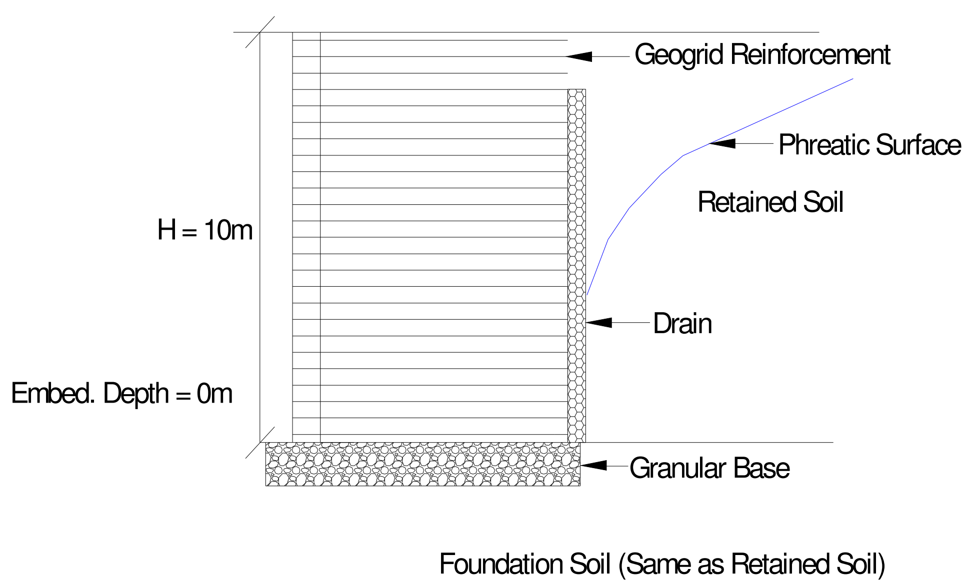


**Figure 6.5: Drain Installation Schematic**
**Figure Not to Scale**

### 6.3 Example Problem Two

The second example problem requires selection of a drain for a geosynthetic reinforced structure (RSS) having the following properties: vertical slope height of 10m, geogrid reinforcement length of 7m and 0.4m vertical spacing and long term design strength, $T_{ltds}$ of 40kN/m, a naturally seeded facing, cohesionless and homogeneous, reinforced and retained soil having permeability, $k = 8.64X10^{-2}$m/day, unit weight of, $\gamma = 20kN/m^3$ and internal angle of friction, $\phi = 30°$. The water table is located at a height of 10m and is indicated by the blue line. Figure 6.6 illustrates the geometry of the slope section.

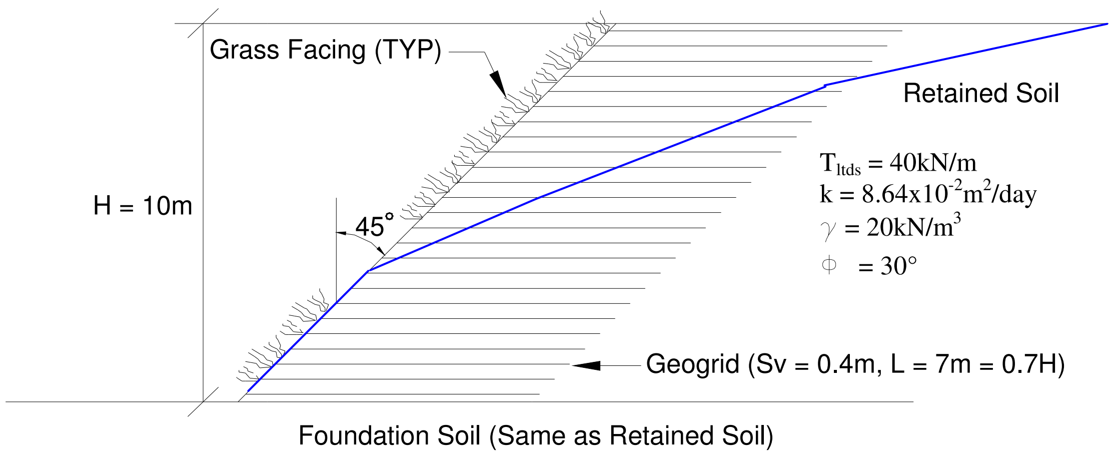


**Figure 6.6: Wall Geometry for Example 2**
**Figure Not to Scale**

**Solution:**

*Step One: Determining the Required Flow Capacity:*

Recall from Table 4.1 in Chapter 4 the following:

**Summary of Seepage Results**

| **Hydraulic Gradient, i (in drain)*** | 1.0 | 0.866 | 0.707 |
|---|---|---|---|
| **Height of Water [m]** | **Flow Rate [$m^3$/day-m]** | | |
| 10 | 0.28 | 0.27 | 0.26 |
| 7.5 | 0.16 | 0.15 | 0.14 |
| 5 | 0.08 | 0.07 | 0.07 |
| 2.5 | 0.03 | 0.02 | 0.02 |

*as defined by discussion in Chapter 4, section 4.3

The vertical height of the slope is 10m with its face oriented at 45°

[$i_{drain}$ = sin(45°) = 0.707] with respect to horizontal therefore the required flow rate is

**0.26 $m^3$/day-m**.

*Step Two: Determine maximum vertical stress drain will experience:*

The maximum vertical stress the drain will experience is:

$$\sigma \approx \gamma z = (20\text{kN/m}^3)(10\text{m}) = \mathbf{200kPa}$$

*Step Three: Determination of Drain Orientation:*

The hydraulic gradient within the drain is:

$$i = \sin \zeta = (\sin 45°) = \mathbf{0.707}$$

*Step Four: Applying Reduction Factors*

From Table 3.2 in Chapter 3 a SD-NW (b) sheet drain with non-woven geotextile facing is chosen as a trial drain. By visual interpolation the approximate flow capacity corresponding to a hydraulic gradient of 0.707 and normal stress of 240kPa is **3.5$m^3$/day-m**. Applying the relevant reduction factors yields:

$$q_{allaw} = q_{ult}\left[\frac{1}{RF_{in} \times RF_{cr} \times RF_{cc} \times RF_{bc}}\right] = 3.5\left[\frac{1}{(1.4)(1.3)(1.3)(1.3)}\right] = \mathbf{1.14m^3/day - m}$$

Because **1.14 $\mathbf{m^3}$/day-m > 0.26 $\mathbf{m^3}$/day-m** the trail drain selection is adequate.

*Step Five: Check Stability*

Figure 6.7 is a safety map generated from ReSSA without a drain installed (i.e., water is present within the reinforced soil zone). The minimum FS indicated by the red region is 0.84 and is considered inadequate as per AASHTO guidelines.

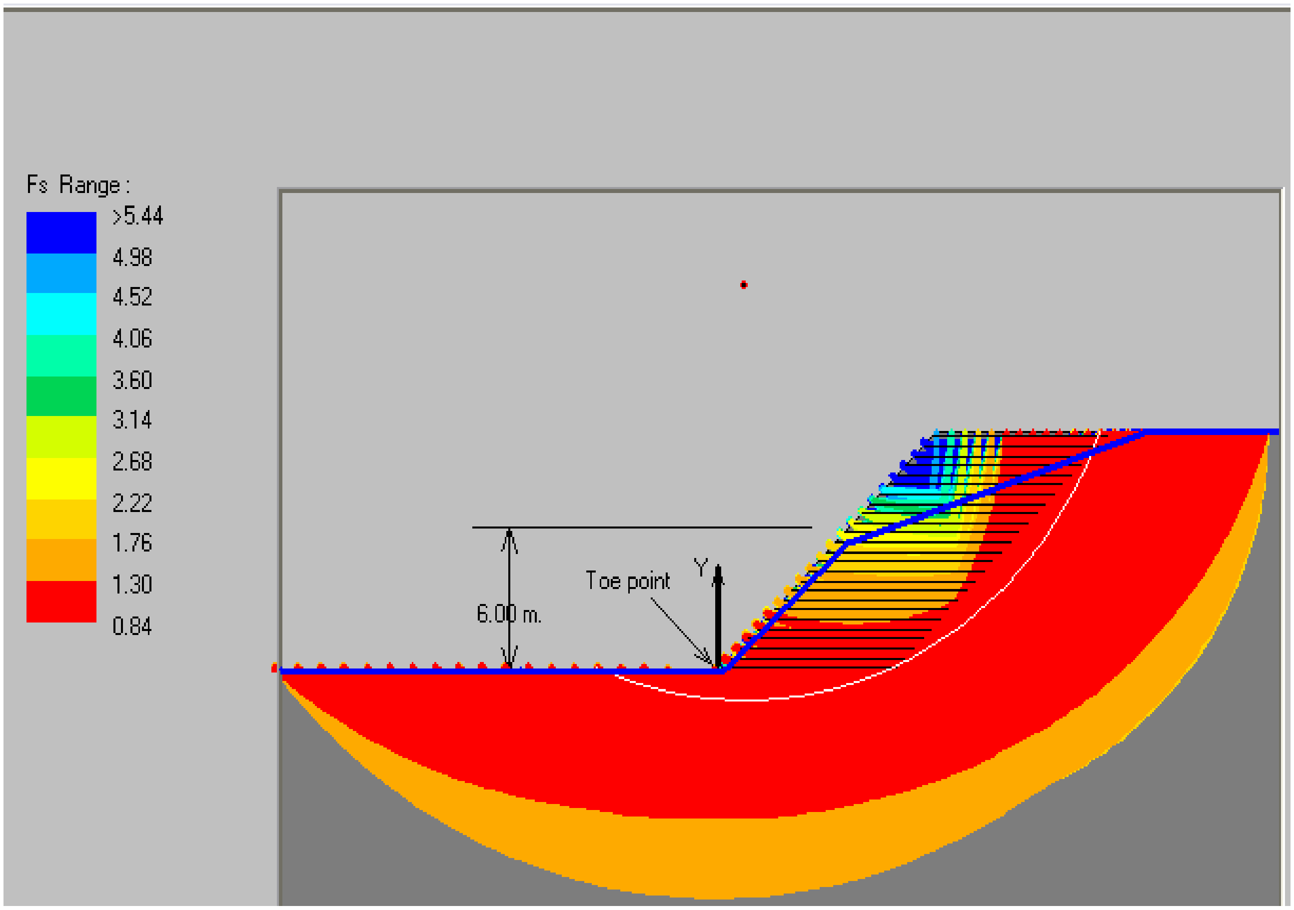


**Figure 6.7: Safety map with effect of water**

To illustrate the effects of installing a drain a second structure was reanalyzed with a drain installed behind the reinforced zone oriented parallel to the slope face. For this particular layout it was also necessary to lengthen the base layer of reinforcement to 12m to attain the desired FS. Figure 6.8 illustrates this stability analysis. Notice that in this case the FS was raised to 1.32 and is considered adequate as per AASHTO guidelines.

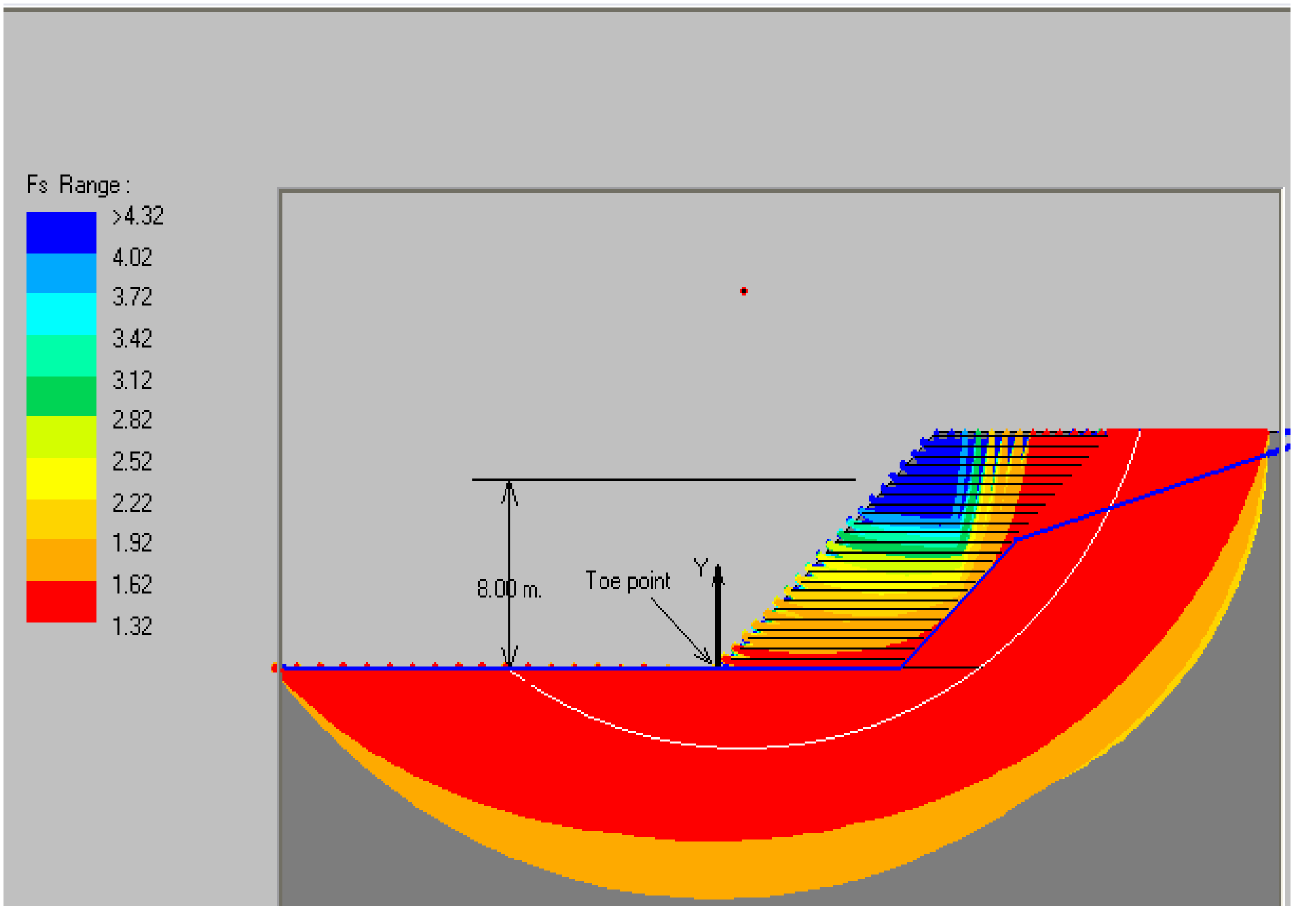


**Figure 6.8: Safety map with drain installed**

### 6.3.1 Drain Installation

As in Example 1, two typical drain layouts are provided to illustrate common installation methods. Again, each method is considered adequate however material availability and experience of the installer will dictate which method is considered the most desirable solution.

Figure 6.9 utilizes a pipe network incorporated with the vertical geosynthetic drain to draw the phreatic surface below and away from the reinforced soil zone similar to that in Figure 6.4. Notice that the drain is installed parallel to the slope face.

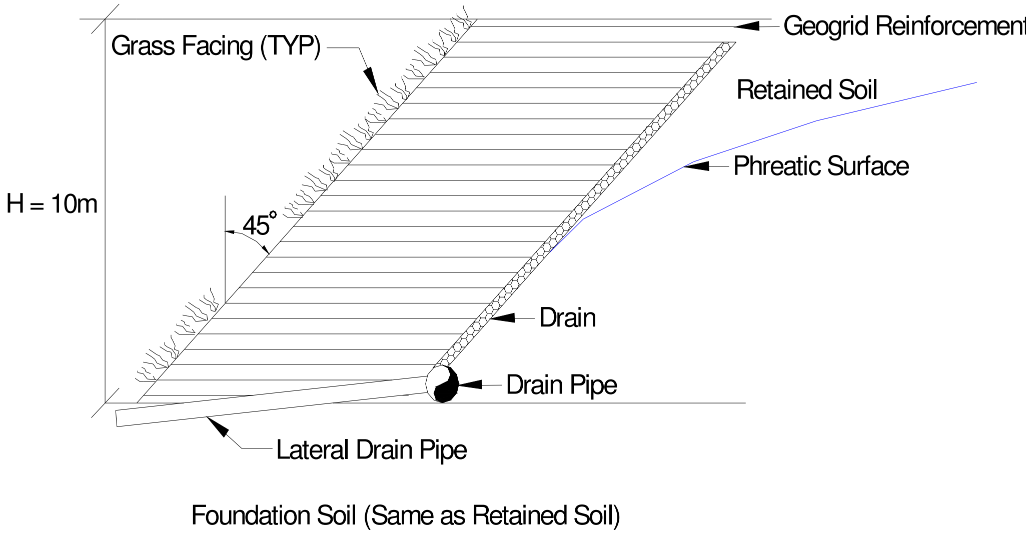


**Figure 6.9: Drain Installation Schematic**
**Figure Not to Scale**

Again, as in Example 1, the pipe network is replaced with a granular base material which transmits water under the base of the reinforced soil zone. Figure 6.10 illustrates this application.

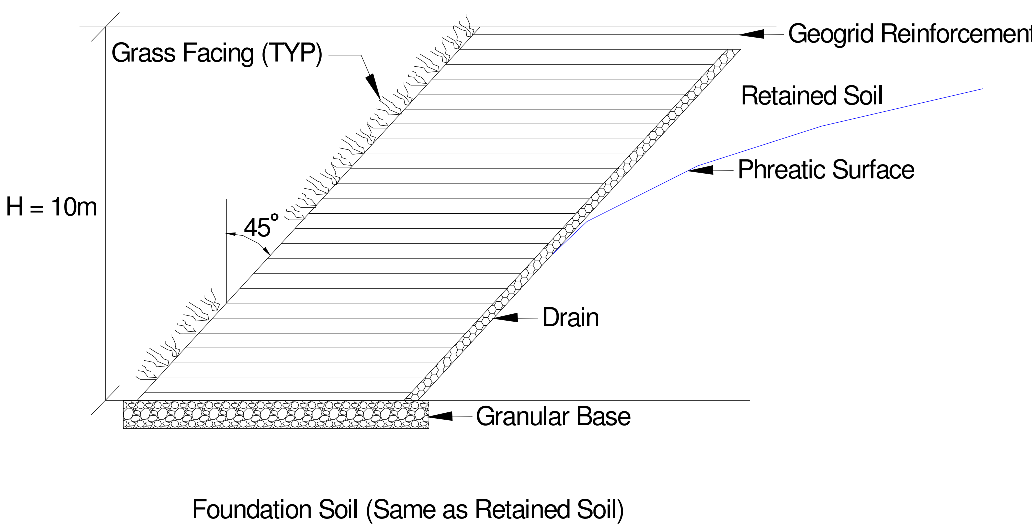


**Figure 6.10: Drain Installation Schematic**
**Figure Not to Scale**

## 6.4 Implications

Example problems one and two illustrate the relative ease of choosing a geosynthetic product to properly drain the reinforced soil zone when a low permeability backfill material is used. The issue of slope stability regarding drain choice must be verified via slope stability analyses to ensure the stability of the reinforced soil structure. The flow capacities designated as the allowable values have suitable Factors of Safety to account for factors that will likely hinder the drains ability to uphold its nominal flow capacity according to Koerner and Koerner (2005).

Chapter 7 provides a summary of the work conducted in generating this thesis. Included are several generalizations that may be derived concerning the effectiveness and results of implementing geosynthetic drains into MSE structures.

Chapter 7

# CONCLUSIONS AND RECOMMENDATIONS

An objective of this thesis was to establish an updated database of the drainage capacities of several geosynthetic drains. Another objective was to propose a procedure in which the usefulness of such drains in mitigating the ill effects of water pressure in the reinforced soil mainly where low permeability backfill material is utilized.

## 7.1 Concluding Remarks and Recommendations

The experimental portion provided representative flow capacities of eight typical geosynthetic drains. In this process, each drain was subjected to a range of consistent normal pressures and hydraulic gradients to provide a baseline material database for comparison and implementation in design. The limits in which each drain is applicable in terms of maximum normal pressure capacity (i.e., maximum height of soil overburden which each drain can withstand) as well as the typical range of hydraulic gradients (related to drain orientation) were also established. This procedure in effect determined the short term flow capacity of the materials under idealized conditions where soil intrusion and long term creep phenomenon were not experimentally measured. In order to account for these reductions in the drain's capacity, a modified method to determine the allowable flow capacity which calibrates the measured flow capacities to the long term performance of the structure was provided in Chapter 6.

A baseline model was established in accordance to AASHTO design procedures where the reinforced backfill, retained and foundation soils possessed consistent properties in terms of unit weight, $\gamma$ friction angle, $\phi$ and permeability, k. The soil and reinforcement properties were held constant to ensure that alterations in reinforcement lengths and strengths would yield no significant changes in stability (i.e., forcing stability changes to occur due to hydrostatic effects). Seepage analyses for several typical slopes were conducted which yielded the phreatic surfaces and subsequent flow rates providing a useful tool to aid in design. The results of the seepage analyses included both geometries of the resulting phreatic surface and the seepage through the retained and reinforced soil masses.

Through parametric studies via Bishop Slope Stability analysis, the effectiveness of implementing the drains was demonstrated in terms of changes in stability (FS) to be compared to the specifications prescribed by AASHTO. In general, based on the integration of seepage and stability analyses, and inclusion of drains the stability (FS) may be increased 30 to 40 percent (compared to conditions where the phreatic surface emerges at the wall face) when a drain is installed behind the reinforced soil zone as illustrated in Chapters 5 and 6.

A comprehensive drain selection procedure was established in Chapter 6 which incorporated the experimental data, seepage and slope stability analyses to develop a baseline design procedure to be utilized when implementing geosynthetic drains in reinforced soil structures. Although not discussed in detail, it is significantly more expensive to both lengthen and strengthen the reinforcement to alternatively raise the FS to acceptable levels than by simply placing a drain behind the reinforced zone.

Other issues that require attention are the possibility of water seepage from surface water runoff into the reinforced soil zone which necessitate procedures not discussed in this thesis. This potential problem exists in cases where the interface directly above the reinforced soil zone is not impervious, therefore allowing the passage of water. Precautionary efforts (illustrated in Figure 7.1) may include installation of a geomembrane directly above the reinforced zone to ensure no surface water will percolate into the reinforced soil zone.

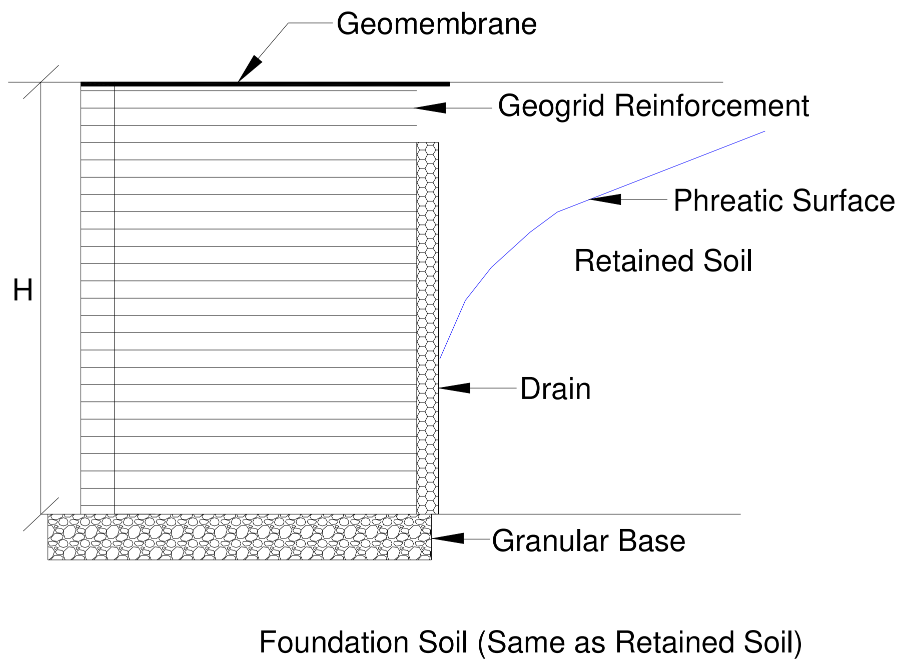


**Figure 7.1: Placement of Geomembrane above Reinforced Soil Zone**
**Figure Not to Scale**

Another pertinent issue that can lead to seepage problems is the inclusion of stormwater drainage pipes within the reinforced zone where the possibility of excessive settlement can lead to damage to the pipe network therefore feeding water directly into the reinforced soil mass. An appropriate stormwater management procedure is illustrated in Figure 7.2.

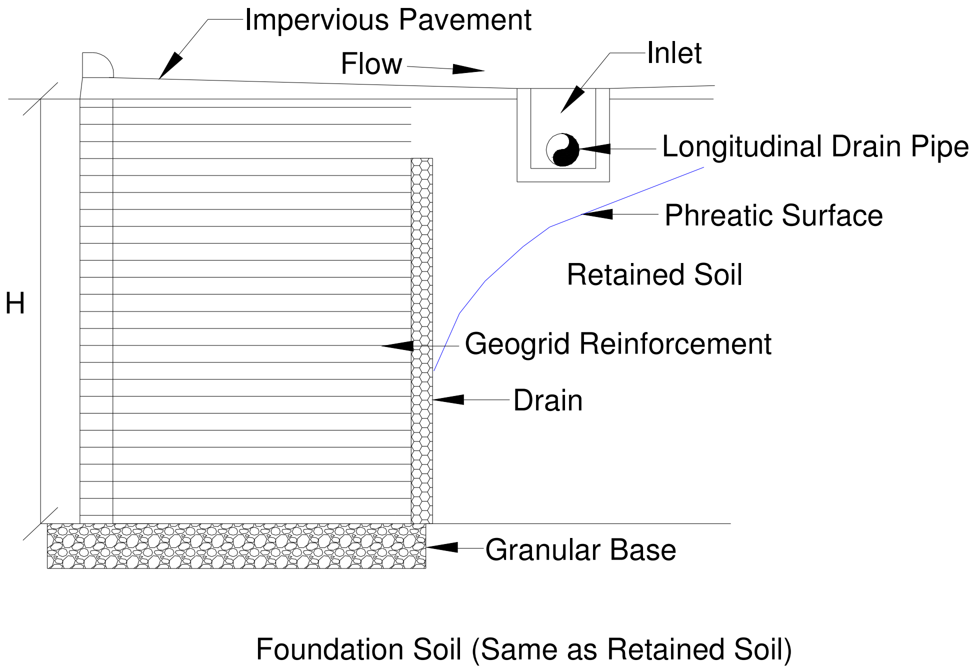


**Figure 7.2: Surface Water Management Method**
**Figure Not to Scale**

As in the design of any geotechnical structure, it is pertinent that the critical site conditions be known in order to ensure proper and safe design and construction procedures. In cases where economics compel implementation of low permeability soil as a reinforced backfill material, the procedures illustrated in this thesis may be utilized however strict quality assurance, quality control (QA/QC) procedures should be adamantly enforced by the geotechnical engineer due to the extreme importance of proper installation and implementation of the materials tested.

**7.2 Topics for further study**

A few topics that were not explored in detail in this thesis due to its limited scope that would justify further study are:

1) To study the effects of long term creep on flow capacity of the drains tested to better analyze the performance of reinforced soil structures toward the end of their lifespan;
2) To perform an in-depth cost analysis comparing the induced cost of lengthening and or strengthening the soil reinforcement to raise the FS to acceptable levels where low permeability backfill material is utilized;
3) To analyze the effects of water in the reinforced zone of slopes with complex geometry (sloping toes, tiered walls, ect.).

## REFERENCES


Federal Highway Administration (FHWA), Earth Retaining Structures, 2005, Washington, DC, March.

Federal Highway Administration (FHWA), Mechanically Stabilized Earth Walls and Reinforced Soil Slopes Design and Construction Guidelines, 2001, Washington, DC, March.

Geo-Slope Office (1998), Geo-Slope Office: Seep/W, Version 4.20, Geo-Slope International Ltd., Calgary, Alberta, Canada, September 1998.

Koerner, G. R. and Robert M. Koerner (2005), Reduction Factors Used in Geosynthetic Design: Part III, GSI White Paper #4, Geosynthetic Institute, Folsum, PA.

Koerner, R. M. (1998), Designing with Geosynthetics, 4th Edition, Prentice Hall, Englewood Cliffs, NJ.

Koerner, R. M. (2004), Handout Materials for Geosynthetics in Reinforced Walls and Slopes, Geosynthetic Institute, Folsum, PA.

Leshchinsky, D., The Power of Software in Geosynthetic Reinforcement Applications: Part III, Geotechnical Fabrics Report, in press, April 2005.

Soong, T.-Y. and Koerner, R. M., (1999), Geosynthetic Reinforced and Geocomposite Drained Retaining Walls Utilizing Low Permeability Backfill Soils, GRI Report No. 24, GSI, Folsum, PA.